

Physical virology: From virus self-assembly to particle mechanics

Pedro Buzón  | Sourav Maity | Wouter H. Roos 

Moleculaire Biofysica, Zernike Instituut, Rijksuniversiteit Groningen, Groningen, The Netherlands

Correspondence

Wouter H. Roos, Moleculaire Biofysica, Zernike Instituut, Rijksuniversiteit Groningen, Groningen, The Netherlands.
Email: w.h.roos@rug.nl

Funding information

Nederlandse Organisatie voor Wetenschappelijk Onderzoek; Stichting voor de Technische Wetenschappen; EU Marie Curie

Abstract

Viruses are highly ordered supramolecular complexes that have evolved to propagate by hijacking the host cell's machinery. Although viruses are very diverse, spreading through cells of all kingdoms of life, they share common functions and properties. Next to the general interest in virology, fundamental viral mechanisms are of growing importance in other disciplines such as biomedicine and (bio)nanotechnology. However, in order to optimally make use of viruses and virus-like particles, for instance as vehicle for targeted drug delivery or as building blocks in electronics, it is essential to understand their basic chemical and physical properties and characteristics. In this context, the number of studies addressing the mechanisms governing viral properties and processes has recently grown drastically. This review summarizes a specific part of these scientific achievements, particularly addressing physical virology approaches aimed to understand the self-assembly of viruses and the mechanical properties of viral particles. Using a physicochemical perspective, we have focused on fundamental studies providing an overview of the molecular basis governing these key aspects of viral systems.

This article is categorized under:

Biology-Inspired Nanomaterials > Protein and Virus-Based Structures
Nanotechnology Approaches to Biology > Nanoscale Systems in Biology

KEYWORDS

mechanical properties, molecular virology, particle mechanics, physical virology, virus self-assembly

1 | INTRODUCTION

Viruses infect cells in all kingdoms of life and, from a physicochemical perspective, can be regarded as molecular machines that have successfully evolved to spread between related organisms. They hijack their host cell's machineries in a highly efficient and minimalistic manner, in order to ensure their propagation. The molecular mechanisms behind the viral life cycle are not only complex, these processes also require a remarkably low number of essential viral components to be successful. The genetic information is stored in all possible configurations known in biology: positive- or negative-sense single-stranded (ss), or double-stranded (ds) RNA or DNA genomes. Viruses are found with very diverse

This is an open access article under the terms of the Creative Commons Attribution License, which permits use, distribution and reproduction in any medium, provided the original work is properly cited.

© 2020 The Authors. *WIREs Nanomedicine and Nanobiotechnology* published by Wiley Periodicals, Inc.

morphologies, but helical and spherical (usually icosahedral symmetry) are the most commonly found morphologies (Crick & Watson, 1956; Zlotnick, 2004).

A characteristic that many viruses have in common, is the ability to form hollow protein shells (capsids), protecting their genome from the external environment. These capsids are either formed without a genome and after completion of the shell the genome is encapsidated with the help of an ATP driven packaging motor, or the capsids are directly formed around the genome (Cuervo, Dauden, & Carrascosa, 2013). In either way, viruses have the remarkable capacity to perform this capsid formation process without any external energy source or specific assistance from the host cell. Under the right conditions, the shell is formed spontaneously by the capsid proteins (CPs), solely due to CP–CP and, in the case of assembly around the genome, CP–genome interactions. Hereby a highly organized supramolecular structure is formed. This process is known as viral self-assembly, and it was first reproduced *in vitro* for a rod-like helical virus, Tobacco mosaic virus (TMV), from its purified genome and CP (Fraenkel-Conrat & Williams, 1955). Twelve years later, the first *in vitro* assembly of an icosahedral virus, Cowpea chlorotic mottle virus (CCMV), was reported (Bancroft & Hiebert, 1967). These early experiments showed that complex viral processes could be studied under controlled non-native conditions, opening new possibilities to investigate their molecular mechanisms from a physicochemical perspective.

Besides their efficient assembly mechanism, viruses also present unique mechanical properties. During the different stages of infection, the viral capsid undergoes changes switching from highly stable states, protecting the genome, to unstable states facilitating genome release. Thus, capsids play a major role in the viral life cycle, and an understanding of their meta-stability and conformational plasticity is key to deciphering the mechanisms governing the successive steps in viral infection. In addition, viral mechanical properties, such as elasticity/deformability, brittleness/hardness, material fatigue, and resistance to osmotic stress, are of particular interest in many areas beyond virology; for instance, soft matter physics, (bio)nanotechnology, and nanomedicine (Cordova, Deserno, Gelbart, & Ben-Shaul, 2003; de Pablo, 2018; Jimenez-Zaragoza et al., 2018; Roos, Bruinsma, & Wuite, 2010).

Both the studies on virus assembly as well as on mechanics have provided essential insights supporting the development of new approaches in nanobiotechnology and nanomedicine (Steele et al., 2017), such as the design of novel broad-spectrum antiviral strategies (Nair et al., 2018; Vahey & Fletcher, 2019; Yang & Lu, 2018), viral-based drug delivery systems (Lam & Steinmetz, 2018), and *de novo* design of synthetic protein cages with potential biotechnological or therapeutic applications (Butterfield et al., 2017; Hernandez-Garcia et al., 2014; King et al., 2012). In this review, we aim to provide an overview of virus self-assembly and viral mechanics, summarizing the latest scientific achievements within these areas. In the first part, we focus on recent studies on the characterization of assembly intermediates and their associated pathways, and proposed strategies to understand genome specificity during packaging. Next, we address recent results obtained from mechanical studies on viral particles, correlating mechanical properties with the different stages of the viral life cycle.

2 | VIRUS SELF-ASSEMBLY

In the simplest scenario of capsid formation, the functional capacity to self-assemble resides in the primary amino acid sequence of the CPs and, hence, the folded structure of the viral protein subunits. Thus, the assembly process is solely driven by protein–protein and, for co-assembly with viral nucleic acids, protein–genome interactions. In 1959, J. D. Bernal wrote in relation to structural units in abiogenesis: “The probability of formation of a highly complex structure from its elements is increased, or the number of possible ways of doing it diminished, if the structure in question can be broken down in a finite series of successively smaller substrates” (Bernal, 1959). This is a statement that can well be applied to virus formation, as viral capsids usually assemble from many, often hundreds, of identical proteins; as a common strategy to achieve the ultimate goal of producing new virions. One of the main challenges of this process is that all viral proteins must encounter and assemble in the crowded environment of cells, where ~200 mg/mL of irrelevant, cellular, proteins are present (Milo, 2013). An additional challenge to capsid formation is the fact that the packaging must be selective to encapsidate the viral genome, discriminating between cellular and viral genetic material, thus ensuring infectivity. Clearly, viruses have found strategies to overcome these challenges, and recent literature has reviewed different aspect of viral assembly (Bhella, 2018; Comas-Garcia, 2019; Fernandez de Castro, Tenorio, & Risco, 2016; Garmann, Comas-Garcia, Knobler, & Gelbart, 2016; Mateu, 2013; Perlmutter & Hagan, 2015a; Twarock & Stockley, 2019; Wang, Mukhopadhyay, & Zlotnick, 2018). The aim of this section is to review the latest scientific achievements in understanding the molecular mechanisms underlying the self-assembly of viruses. Particularly, we

focus on results of the characterization of new assembly intermediates and their associated pathways, and the latest discoveries in the viral mechanisms that provide genome specificity during packaging.

2.1 | Pure capsid protein assembly pathways and their intermediates

The self-assembly of a set of viral proteins into a regularly shaped capsid involves a fine-tuned range of interactions between the capsid proteins to create this highly ordered, symmetrical, supramolecular structure. The mechanism of assembly of viral capsids was initially characterized for the procapsid of P22 by two steps: nucleation-and-growth/elongation (P. E. Prevelige Jr., Thomas, & King, 1993). First, a nucleus must be formed. A nucleus is defined as the smallest intermediate of assembly with more than 50% probability to grow instead of disassembling (Perlmutter & Hagan, 2015a). Next, the nucleus size is increased by the sequential addition of protein subunits, that is, the growth phase (Figure 1a,b). In the particular case of spherical viruses, the end of the growth phase is completion or closure of the capsid. As this closure shows significant differences in kinetics and stability compared to the growth phase, it can be considered as a separate step. Thus, a three-step mechanism was proposed and this distinction is now often used, that is: nucleation, growth, and completion (Endres & Zlotnick, 2002; Hagan, 2014; Hagan & Elrad, 2010; Michaels et al., 2017; Nguyen, Reddy, & Brooks 3rd., 2007; Zandi, van der Schoot, Reguera, Kegel, & Reiss, 2006).

In a simplified view, assembly is a spontaneous process driven by weak protein–protein interactions on the order of several $k_B T$ (Ceres & Zlotnick, 2002). These weak attractive interactions are mainly of a hydrophobic nature (del Alamo & Mateu, 2005; Kegel & van der Schoot, 2006) and are able to overcome the entropic penalty associated with forming the highly organized capsid structures. Coarse-grained models indicate that the growth phase proceeds as a downhill process, while completion is rate-limited due to steric effects (Hagan, 2014; Michaels et al., 2017; Nguyen et al., 2007; Figure 1a). The latter is even thermodynamically unfavorable when only looking at the loss in flexibility upon capsid closure (Nguyen et al., 2007). Under assembly conditions, small intermediates are transient and the formation of nuclei are rare events (Endres & Zlotnick, 2002; Hagan & Elrad, 2010), making them difficult to characterize. On the other hand, large intermediates are reasonably stable, and easier to identify. However, the large number of protein subunits per capsid (for icosahedral capsids typically specific multitudes of 60, as described by the quasi-equivalence theory and the related triangulation number [Caspar & Klug, 1962]) leads to limitations in the experimental resolution. For such large numbers of subunits, it is hard to discriminate complete capsids from capsids missing a few subunits. Indeed, both nucleation and completion are very challenging processes to investigate, which explains why only a limited amount of experimental studies have been reported on this topic.

Another characteristic of virus self-assembly studies is the fact that assembly/disassembly reactions are typically triggered under controlled conditions. The capability of CPs to assembly is frequently tuned by changing solvent conditions such as pH, salt concentration, or mild concentrations of denaturant agents. Typically, denaturant agents such as urea and guanidinium hydrochloride are used to trigger capsid disassembly, while keeping CPs in their folded state. Changing pH can also be effective at producing individual protein subunits from viral capsids. Then, assembly reactions are usually initiated by removing the denaturant agents and tuning salt concentration and/or pH to allow CPs to reassemble into capsids.

The *in vitro* assembly and disassembly of one of the simplest virus particles known, the minute virus of mice (MVM), has been recently characterized using a combination of atomic force microscopy (AFM) and transmission electron microscopy (TEM; Medrano et al., 2016). MVM forms $T = 1$ icosahedral capsids of 25 nm made of only 60 CPs, which arrange as trimeric subunits (Figure 1b). The whole range of particle sizes were found in this study (Medrano et al., 2016), from complete capsids, via large incomplete capsids, to small capsid intermediates (Figure 1c). Complete capsids were analyzed separately according to their capability to be permeable to uranyl ions, as characterized by TEM experiments. Figure 1c shows the disassembly (left graph) and assembly (right graph) evolution of intermediates to and from complete capsids over time. In all cases, both large and small intermediates are only populated in low numbers, and hence, transient. This is indicative of a highly cooperative process. MVM assembly represents a distinct experimental example of the nucleation-and-growth pathway introduced above; where capsid formation can be simplified as the sum of equilibria by which individual protein subunits are sequentially added to the growing structure until completion (Figure 1b). For MVM, and also in the following set of descriptions, we are considering the formation of empty capsids, that is, without accounting for the contribution of the genome to the assembly process. The study of such simplified systems, empty virus-like particles (VLPs), has been proven to be instrumental in characterizing viral assembly. This is particularly relevant for viruses such as hepatitis B virus (HBV), which produces *in vivo* around 90% of the viral

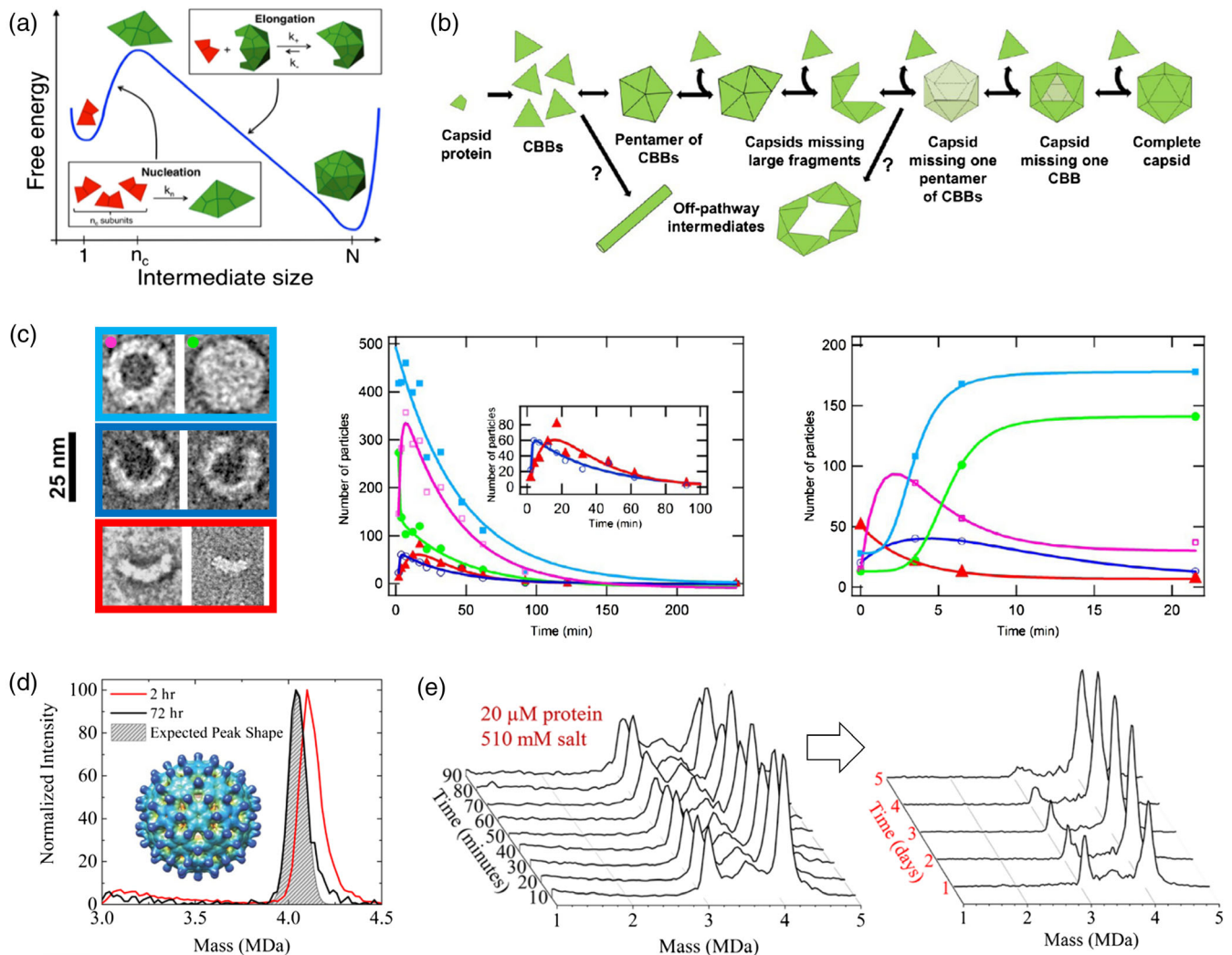


FIGURE 1 Assembly of empty particles through the nucleation, growth, and completion pathway. (a) Schematic representation of the free energy profile of the nucleation-and-growth/elongation pathway: first, nuclei are formed; then, the reaction proceeds downhill until the complete closure of the capsid. (Reprinted with permission from Michaels, Bellaiche, Hagan, and Knowles (2017)). (b) Self-assembly model proposed for MVM empty capsids based on the sequential addition of trimeric subunits, or CBBs (capsid building blocks). (Reprinted with permission from Medrano et al. (2016)). (c) MVM particles imaged by TEM (left): light blue, Types I + II particles (complete capsids); green, Type I (complete capsids in basal state); magenta, Type II (complete rearranged capsids); blue, Type IIIA (large incomplete capsids); red, Type IIIB (smaller incomplete capsids). Progression of the total number of particles during disassembly (left graph) and assembly (right graph) over time. (Reprinted with permission from Medrano et al. (2016)). (d) CDMS spectrum in the region of 3.0 to 4.5 MDa after 2 hours (red trace) and 72 hours (black trace) from the initiation of the HBV assembly reaction with 5 μM CP dimers in 210 mM ammonium acetate. The gray shaded area shows the expected peak for the $T = 4$ capsids. Inset, representation of the HBV $T = 4$ capsid. Reprinted with permission from (Lutomski et al., 2017). (e) Time-resolved CDMS spectra showing the progression of capsid assembly over the first 90 min (left) and in the scale of days (right), for an assembly reaction containing an initial CP dimer concentration of 20 μM in 510 mM ammonium acetate. (Reprinted with permission from Lutomski et al. (2018)). CBB, capsid building block; CDMS, charge detection mass spectrometry; CP, capsid protein; MVM, minute virus of mice; TEM, transmission electron microscopy

particles as empty particles (Sakamoto et al., 1983). In this context, Utrecht and coworkers used native Mass Spectrometry (native MS) to study the nucleation mechanism of empty HBV particles (Utrecht, Barbu, Shoemaker, van Duijn, & Heck, 2011). HBV forms $T = 4$ icosahedral particles, of 120 CP dimers, as the major product of assembly (Crowther et al., 1994; Stannard & Hodgkiss, 1979), with an expected mass of ~ 4 MDa (Utrecht et al., 2008).

Using a different MS approach, the mechanisms behind the completion phase of HBV assembly was studied (Lutomski et al., 2017) by applying charge detection mass spectrometry (CDMS). Using single-particle CDMS, the authors identified a novel mechanism by which HBV particles seem to experience overgrowth, and then slowly relax to

the final $T = 4$ structure (Lutomski et al., 2017; Figure 1d). These results suggest an unexpected completion pathway for HBV, in which late intermediates are bigger in size than the complete and closed capsid. Instead of particles missing CP subunits, HBV forms slightly overgrown particles of >4 MDa (>120 CP dimers) that seem to be kinetically favorable. Then, a spontaneous proofreading process, which occurs on a time scale much longer than that of the initial assembly reaction, appears to correct overgrown structures to form icosahedral capsids (Lutomski et al., 2017). In a later study, additional CDMS experiments were performed to track HBV assembly at different ionic strength conditions (Lutomski et al., 2018). At high salt concentration (510 mM ammonium acetate) the assembly proceeds relatively fast (less than a minute), due to screening of the electrostatic repulsive interactions between CPs. However, in this situation approximately half of the assembly reaction ends in intermediates of <120 CP dimers (between 3 and 4 MDa; Figure 1e). Potentially, these are kinetically trapped intermediates formed by defective growing capsids that arise from the stronger CP–CP association energy imposed by the experimental conditions. This is in agreement with the expectations of the strengthening of CP–CP interactions by increasing salt concentration, as these interactions are modulated by competing actions of hydrophobic attractive patches, and electrostatic repulsive amino acid residues (del Alamo & Mateu, 2005; Kegel & van der Schoot, 2006). Interestingly, some of these large intermediates are part of a successful assembly pathway, since some of them evolve to full capsids, again, on a much longer time scale (Lutomski et al., 2018; Figure 1e).

Similar results have been found using single-particle resistive-pulse sensing (Zhou et al., 2018), at even higher salt concentration of 1.0 M. The authors identified a shift in size for late intermediates, from 105–113 CP dimers to 114–117 CP dimers, after a two-day reaction; consistent with mass spectrometry data (Lutomski et al., 2018). In addition to these findings, it has been observed that for HBV disassembly experiments a spherical structure with a single hole has a low probability to be formed (Lee et al., 2017). However, the results presented do not provide an explanation for the observation that HBV intermediates are stalled between 3 and 4 MDa (90–120 CP dimers) under increasing ionic strength, while up to 3 MDa the reaction occurs fast. Nevertheless, these experiments shed light on the fact that a multitude of pathways are allowed during viral assembly; pathways that are partially determined by external conditions. Moreover, new insights into the complexity of the completion phase of spherical viruses are provided.

2.2 | Effect of the RNA genome on assembly pathways

We have seen how the assembly pathway of empty VLPs can be modulated by tuning the association energy between CP subunits. We now consider the role of the genome, which can redefine the viral assembly pathway. Specially, we focus on the mechanisms that lead to the assembly of small spherical viruses around (ss) genomes. The viral assembly around single-stranded genomes is widely accepted to be thermodynamically driven by electrostatic interactions between a negatively charged genome and positively charged CPs (H. K. Lin, van der Schoot, & Zandi, 2012; Sikkema et al., 2007; Sivanandam et al., 2016; Zlotnick, Aldrich, Johnson, Ceres, & Young, 2000). For instance, CPs of many negative-sense ssRNA viruses interact with RNA via a positively charged cleft (Ruigrok, Crepin, & Kolakofsky, 2011), while for a variety of positive-sense RNA viruses, CPs present a flexible arginine-rich motifs (Speir, Munshi, Wang, Baker, & Johnson, 1995). Taking this into account, it is now clear that the relative balance between CP–CP and CP–genome interaction energies, will determine the assembly path. Focusing on these parameters, two different pathways have been proposed (Elrad & Hagan, 2010; Perlmutter, Perkett, & Hagan, 2014; Zlotnick, Porterfield, & Wang, 2013): (a) in the first one, a nucleation structure with defined CP–CP interactions is formed on the genome, and the nucleus grows by the sequential addition of subunits; (b) in the second one, subunits absorb fast and en masse onto the genome with loose or absent CP–CP interactions, and then the irregular complex reorganizes into a well-ordered, filled capsid. The former resembles the nucleation-and-growth mechanism described for empty capsids, and is associated with strong CP–CP interactions. The latter pathway instead, is preferentially followed by viruses with stronger CP–genome interactions (Figure 2a).

Cowpea chlorotic mottle virus is an icosahedral, ssRNA, plant virus that forms $T = 3$ capsids by the association of 90 CP dimers. CCMV *in vitro* assembly has been characterized using a two-step assembly reaction, as recently reviewed (Garmann et al., 2016). It assembles by the en masse pathway and the two-step assembly reaction proceeds as follows: first, CPs bind to the genome forming amorphous particles at low ionic strength and neutral pH; then, the pH is lowered to enhance CP–CP contacts and regular $T = 3$ filled VLPs are formed. Chevreuril and coworkers followed this assembly on ssRNA using time-resolved small angle X-ray scattering (Chevreuril et al., 2018). At neutral pH, the authors identified stable intermediates of around 75 CP subunits in size, less than the expected 90 dimers that would form a complete capsid. Following the number of genome-bound subunits per intermediate over time, a single exponential

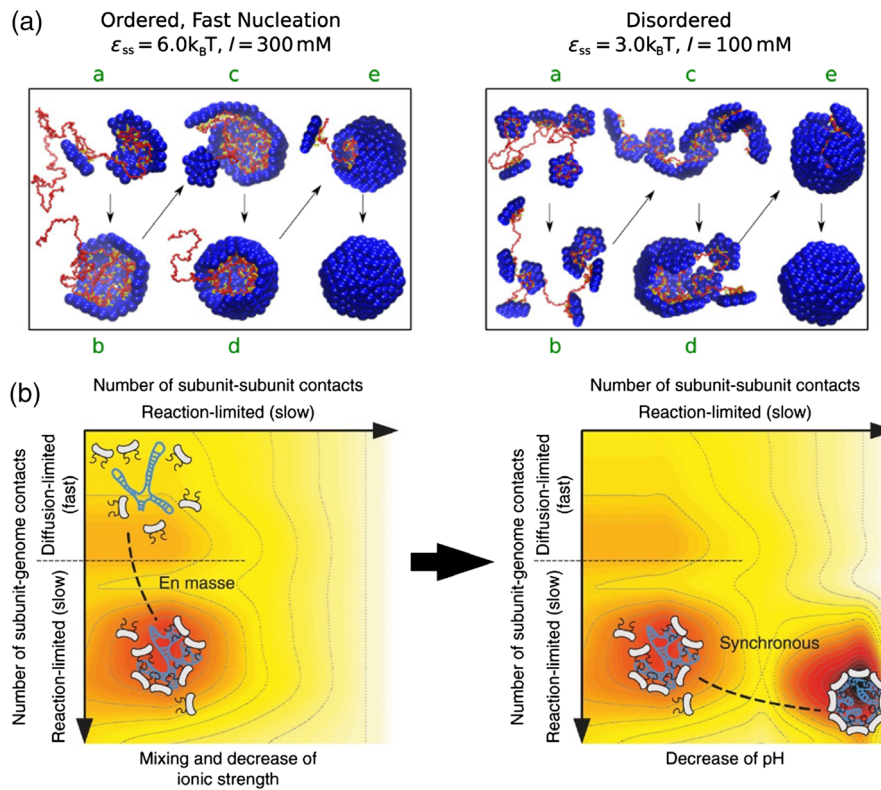


FIGURE 2 Energetics of the self-assembly of genome-filled capsids. (a) Snapshots obtained from simulations of the nucleation-and-growth (ordered) and en masse (disordered) assembly pathways by tuning the parameters ϵ_{ss} (protein–protein interaction strength) and I (ionic strength). (Reprinted with permission from Perlmutter et al. (2014)). (b) Free energy landscape scheme of CCMV assembly modulated by the change in ionic strength (left) and pH (right). Left, the graph shows the formation of a CP-genome amorphous complex through the en masse pathway, driven by CP–genome interactions. Right, the amorphous complex rearranges into a full capsid by the increased strength of CP–CP interactions through the synchronous pathway. Dark colors delimit areas of low free energy, while light colors represent high free energies regions. (Reprinted with permission from Chevreuril et al. (2018)). CCMV, Cowpea chlorotic mottle virus; CP, capsid protein

growth function revealed a genome binding time τ_{bind} of ~ 28 ms. Analogously, tracking the radius of gyration over time, indicative of the compactness of the formed structures, the time scale of forming the final compact structure τ_{struc} was determined to be ~ 48 s; three orders of magnitude higher than τ_{bind} . This points toward an en masse pathway, in agreement with the expected CCMV assembly mechanism (Figure 2a, right panel). However, the authors report a moderate CP–genome binding energy of $\sim 7k_B T$, which is unexpectedly low, because the en masse assembly mechanism is associated with strong CP–genome interactions. Moreover, the same analysis was carried out when lowering the solution pH to 5.2. In this case, the process was found to take place over a much longer time frame ($\sim 3,000$ s), with $\tau_{\text{bind}} \approx \tau_{\text{struc}}$. Interestingly, this suggests that the system proceeds through a synchronous mechanism, where the evolution of the particle toward icosahedral symmetry and the addition of new CP dimers to the growing capsid occur simultaneously; in agreement with coarse-grained simulation (Perlmutter et al., 2014). Furthermore, repeating pH 5.2 experiments at different temperatures, a binding activation energy of $20k_B T$ was obtained, indicative of a reaction-limited process. Figure 2b shows a schematic representation of the free energy landscape of the CCMV assembly around ssRNA. As can be appreciated from the figure, the assembly reaction can be characterized in terms of CP–CP and CP–genome contacts. In this particular case of an en masse and synchronous pathway, Figure 2b visualizes how the driving force is first due to CP–genome interactions, and second led by CP–CP interactions.

2.3 | Genome specificity scenarios

Genome specificity is one of the most intriguing features of viruses. It is revealed in very diverse ways for different viruses, sometimes exhibiting the finest and most precise mechanisms of nature. As we have already discussed, the

electrostatic interactions formed between genome and CPs, are a major driving force in the viral assembly. However, these electrostatic interactions were early proven to be rather nonspecific, as demonstrated by *in vitro* assembly experiments using heterologous nucleic acids and even negatively charged polymers to generate VLPs (Bancroft, Hiebert, & Bracker, 1969; Hohn, 1969). Therefore, considerations of electrostatics alone do not provide an explanation for the remarkable characteristic of viruses to recognize their own genome; instead, it raises more questions.

2.3.1 | Packaging signals

The well-studied plant virus, TMV, forms ~18 nm diameter rod-like helical particles of ~300 nm in length composed of two components: the capsid protein (CP) and a single molecule of its ssRNA genome. TMV exhibits a very robust mechanism to control the packaging process. The TMV genome encodes a packaging or nucleation signal, which provides the desired specificity for CP capsomers to be recognized as the initiating point for assembly. TMV packaging signal (PS) is a short sequence that forms a loop of a well-defined hairpin like-structure (Zimmern, 1977; Zimmern & Butler, 1977). Somehow, CP capsomers (CP disks) are able to discriminate this region from many similar stem-loops present in the TMV genome, which in principle is solely due to the higher affinity of the TMV CP for this PS. The robustness of this PS strategy is demonstrated when *in vitro* assembly is performed on modified genomes including two to four PSs (Eber, Eiben, Jeske, & Wege, 2015). In this scenario, wild-type TMV particles can be distorted and form non-linear particles. In particular, “tetrapods” are formed when four PSs are included in the ssRNA sequence. The TMV PS is so strong and specific that it can also be inserted into heterologous RNA leading to efficient packaging of any RNA into wild-type TMV capsids. These results highlight how PS can regulate the initiation of assembly and selectivity in virology. Similarly, human immunodeficiency virus 1 (HIV-1) selectively packages its genomic RNA during virus assembly. Although the HIV-1 recognition mechanism is not fully understood (Comas-Garcia, Davis, & Rein, 2016), recent studies suggest that the interaction of Gag (viral structural protein) with the PS of HIV-1 has a nonelectrostatic component, which confers the desired specificity (Comas-Garcia et al., 2017; Comas-Garcia et al., 2018).

TMV and HIV-1 assembly exemplify the robustness of encoding a well-defined PS to trigger specific and selective capsid formation, while the rest of the genome does not seem to play a sequence-specific role during the assembly process. However, viruses do not always show a clear single PS on their genome driving the assembly; this is particularly valid for spherical ssRNA viruses. Instead, a new strategy has been proposed to explain genome specificity of these viruses, highlighting the active role of the whole viral genome during packaging. It relies on the fact that multiple and dispersed specific interactions between the genome and the CPs take place during capsid assembly. Thus, multiple, dispersed PSs are represented by multiple secondary structure elements with CP recognition features. Based on these premises, a model of PS-mediated assembly was applied using Gillespie algorithm simulations, to characterize the kinetics and assembly efficiency of this group of spherical viruses (Dykeman, Stockley, & Twarock, 2013a, 2014). The model relies on simple rules: CP capsomers interact with dispersed PSs on the genome at different rates depending on CP–PS affinity; and the CP–CP capsomer interaction rates are determined by the free energy of CP–CP bonds. In addition, protein concentration must increase during assembly, known as protein ramp, as has been reported for bacteriophage Q β assembly *in vivo* (Eigen, 2000). This novel theoretical framework solves the protein folding equivalent of Levinthal’s Paradox for virus self-assembly and explains the genome specificity and cooperativity of the process (Dykeman et al., 2014). The extent of the model has been recently reviewed by the authors (R. Twarock, Bingham, Dykeman, & Stockley, 2018; R. Twarock & Stockley, 2019). Furthermore, similar results have been found by coarse-grained particle-based simulations (Perlmutter & Hagan, 2015b). The authors identify more compact intermediates of assembly when adding PSs to the system; finding that a combination of one high affinity PS and several low affinity PSs leads to the highest assembly yields.

The suitability of the PS-mediated assembly model has been fully tested on the well-characterized bacteriophage MS2, a positive-sense ssRNA virus with a sphere-like capsid of icosahedral symmetry. The MS2 genome was scrutinized using SELEX (systematic evolution of ligands by exponential enrichment), in order to identify protein-binding sites on RNA (Figure 3a), combined with Hamiltonian path analysis (HPA) to predict aspects of genome organization (Figure 3b; Dykeman, Stockley, & Twarock, 2013b). Dispersed PSs were also identified on the MS2 genome using crosslinking immunoprecipitation and desorption/ionization mass spectrometry (Rolfsson et al., 2016), showing excellent agreement with PSs positions proposed in Dykeman et al. (2013b). In parallel, the asymmetric cryo-EM reconstruction of MS2 particles at 8.7 Å resolution (Koning et al., 2016), and the subsequent reconstruction at 3.6 Å (Dai et al., 2017) revealed the structures of both the protein shell and the asymmetric genome arrangement. The 15 high affinity

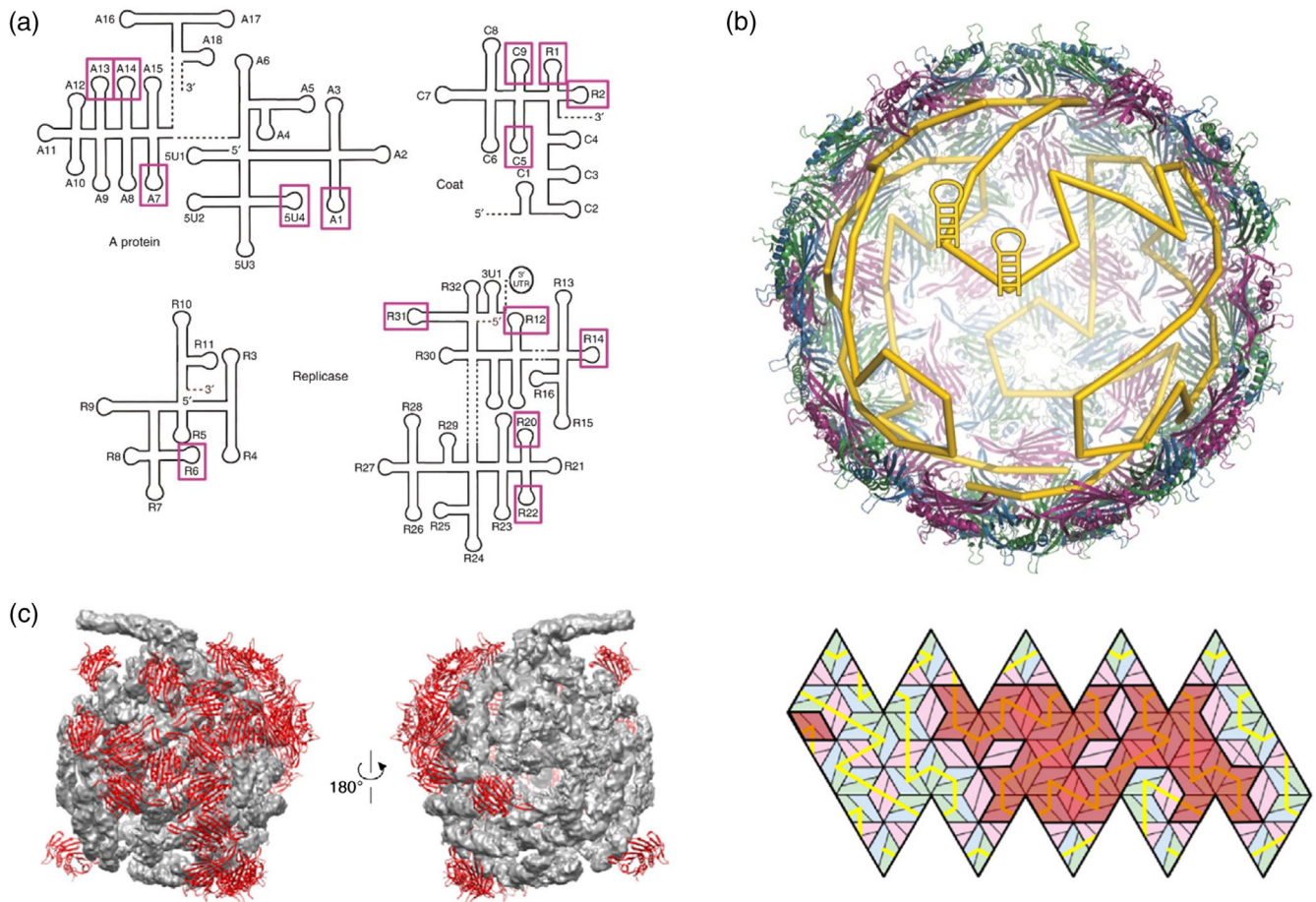


FIGURE 3 MS2 assembly predicted by the PS-mediated model. (a) Representation of the MS2 genome with the 15 stem-loops (magenta boxes) found in the asymmetric cryo-EM reconstruction (Dai et al., 2017), and previously predicted to be PSs via HPA (Dykeman, Stockley, & Twarock, 2013). (b) Hamiltonian path representation of MS2 genome arrangement connecting binding sites inside the MS2 capsid. (a and b reprinted with permission from Twarock, Leonov, and Stockley (2018)). (c) Left, identified PSs by cryo-EM reconstruction of MS2 particles at 8.7 Å resolution (Koning et al., 2016) are predominantly located in one half of the capsid; in agreement with predictions (right; Dykeman et al., 2013), showing that the positions of PSs bound to CPs (red rhombs) are also mainly located in one half of the capsid inner surface. (c reprinted with permission from Twarock, Bingham, et al. (2018)). CP, capsid protein; HPA, Hamiltonian path analysis; PS, packaging signal

PSs predicted by Dykeman et al. (2013b), and therefore expected to be conserved in every viral particle, are found in contact with CP capsomers in both MS2 cryo-EM reconstructions. In addition, the asymmetrical arrangement of the MS2 genome derived from the HPA is also seen in the mentioned EM structures (Figure 3c; R. Twarock, Leonov, & Stockley, 2018). These remarkable results corroborate the suitability of the PS-mediated assembly model combined with HPA to characterize MS2 assembly. Furthermore, disperse PSs have been recently identified in other viruses, such as satellite tobacco necrosis virus (Patel et al., 2015; Patel et al., 2017), human Parechovirus (Shakeel et al., 2017), hepatitis C virus (Stewart et al., 2016), and HBV (Patel et al., 2017). Thus, even though PSs may play distinct roles in different viruses during the assembly process, all of them could share the same basic mechanism: disperse sites in their (pre) genomes with affinity for their associated CPs drive the efficient formation of capsids with the optimal geometry.

2.3.2 | Overall RNA topology effects

Packaging signals are not the only features to take into account when studying genome specificity during viral self-assembly. Concomitant with PS-mediated studies, efforts have been devoted to decipher the role played by nonspecific electrostatic interactions between CPs and viral genomes, and by physical properties of RNA genomes such as length,

degree of branching, and stiffness. Such studies are motivated by experimental observations for certain viruses that point toward a marginal or nonexistent role of sequence specificity. For instance, in vitro assembly experiments have shown that CP of HBV has no clear preference packaging genomic RNA over heterologous RNA of equal length (Porterfield et al., 2010). Similarly, competition assays in which a limited amount of CCMV proteins is mixed with an equal amount of CCMV and Brome mosaic virus (BMV) genomes, showed that CCMV particles are preferentially assembled around BMV RNA, that is, BMV RNA outcompetes CCMV cognate RNA for CCMV CPs (Comas-Garcia, Cadena-Nava, Rao, Knobler, & Gelbart, 2012). This example highlights the impact of RNA topology, as BMV RNA has a more compact arrangement than the cognate RNA of CCMV (Erdemci-Tandogan, Wagner, Schoot, Podgornik, & Zandi, 2014). In particular, it was proposed that an increasing degree of RNA branching produces a gain in assembly efficiency. Specifically, the RNA with larger number of branching junctions, and therefore with a more compact arrangement, exhibits an advantage under competitive packaging conditions.

The observation that more compact RNA structures could lead to more efficient packaging is supported by simulation studies (Perlmutter, Qiao, & Hagan, 2013; Singaram, Garmann, Knobler, Gelbart, & Ben-Shaul, 2015) and mean-field theory calculations (Erdemci-Tandogan et al., 2014; Erdemci-Tandogan, Wagner, van der Schoot, Podgornik, & Zandi, 2016; Li, Erdemci-Tandogan, Wagner, van der Schoot, & Zandi, 2017). These studies show that the amount of RNA bases that can be packed by a given protein shell depends on how efficient RNA secondary structures are formed. In fact, it has been demonstrated that nonviral RNA is in general less compact than the viral RNA genomes (Figure 4a), when comparing RNA molecules with the same length and similar amount of base-pairing (Ben-Shaul & Gelbart, 2015; Bruinsma, Comas-Garcia, Garmann, & Grosberg, 2016; Gopal, Zhou, Knobler, & Gelbart, 2012; Yoffe et al., 2008). Perlmutter and coworkers also performed coarse-grained particle-based simulations for several specific viruses, considering genome secondary structure and total charge of CPs (Perlmutter et al., 2013). Figure 4b shows how these predictions compare to values of charge ratio (genome charge/CP charge) when genome base-pairing is included. The concepts of nonspecific electrostatic interactions and RNA branching provide further insights into our understanding of genome packaging by considering intramolecular charge repulsion compensation, between CPs and ssRNA, and by accounting for the compact conformations of viral genomes. Therefore, these findings indicate that sequence-specific protein-RNA interactions are not the only mechanism that leads to genome specificity. In the next section, we will discuss how RNA topology also influences the stability and mechanical properties of the formed viral particles, as a complementary approach to understand viral packaging.

In order to further investigate the suitability of the above presented theories, Beren and coworkers recently performed in vitro assembly experiments using CCMV CPs and polyU, an ssRNA molecule only composed of uridylic acid that lacks secondary structure (Beren et al., 2017). Following the same strategy reported by (Comas-Garcia et al., 2012), head-to-head competition experiments were carried out to test the preference of CCMV CP for its cognate RNA over the less compact and unfolded polyU molecules. Surprisingly, competition assays showed that polyU outcompetes viral RNA for CP. Even when using BMV RNA, which outcompetes CCMV cognate RNA, polyU wins the assembly competition for CCMV CPs. These intriguing results also lead to $T = 2$ -sized particles (~22 nm) when polyU is packed by CCMV CPs, in contrast with the well-characterized $T = 3$ of CCMV wild-type particles (28 nm; Figure 4c, left graph). Somehow, polyU molecules of ~3,000 nucleotides, which is a similar length to CCMV RNA and BMV RNA, form smaller VLPs than wild-type particles, even though their 3D size (hydrodynamic radius) is larger, in disagreement with the RNA topology theories presented above. In addition, the authors also find that the order in which RNA molecules are added to the assembly reaction critically determines the outcome of the experiments (Beren et al., 2017), as opposed to the observations made by (Comas-Garcia et al., 2012) for other RNA molecules. Figure 4c shows the size distribution of VLPs obtained from the competitive self-assembly reactions when BMV RNA (B1) and polyU are added simultaneously (left graph), and when the order of mixing was altered (right graph; Beren et al., 2017). These experiments show for the first time, how a linear polymer (polyU) outcompetes branched ones (viral RNA), while keeping all other chain quantities equal, and are not what would be predicted by the previously mentioned experimental work, simulations and theoretical calculations.

These observations emphasize that the role of RNA topology in the self-assembly of spherical ssRNA viruses is still not fully understood. In this context, Van der Schoot and Zandi already suggested the important role of balancing Kuhn length and linear charge density distribution in order to predict the free energy gain of polymer encapsulation (van der Schoot & Zandi, 2013). The Kuhn length of ssRNA at neutral pH in the presence of monovalent salt can vary between 1 and 2 nm (H. Chen et al., 2012), while that of dsRNA is bigger than 120 nm (Abels, Moreno-Herrero, van der Heijden, Dekker, & Dekker, 2005; Kebbekus, Draper, & Hagerman, 1995), that is, dsRNA is much stiffer than ssRNA. Moreover, a further difference between single-stranded and double-stranded RNA molecules is the linear charge density, which is

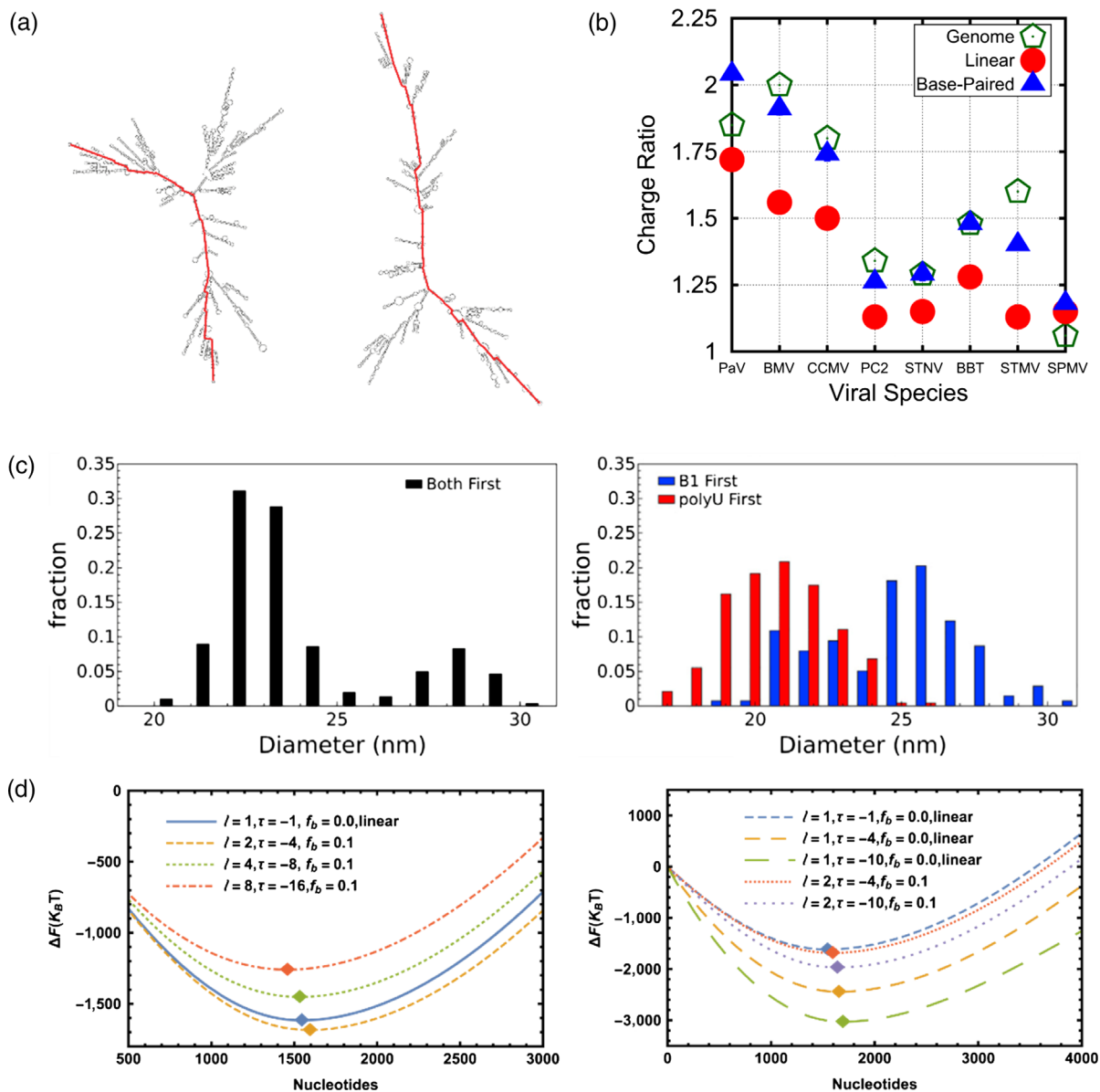


FIGURE 4 Contributions of RNA topology to viral assembly. (a) Comparison of the secondary structure of BMV RNA (left structure), and a nonviral random RNA sequence (right structure) with equal numbers of bases and base proportions. The maximum ladder distance, that is, the number of basepairs crossed along the trajectory between the two most distant hairpin loops, of both structures are 207 and 354, respectively, represented as red lines. (Reprinted with permission from Ben-Shaul and Gelbart (2015)). (b) Plot of the charge ratios (genome charge/CP charge) calculated for several viruses (green pentagons), and predicted for linear polyelectrolytes (red circles) and model nucleic acids with 50% base-pairing (blue triangles). (Reprinted with permission from Perlmutter et al. (2013)). (c) Size distributions of the VLPs formed from competitive self-assembly. Left, competition assay in which polyU (~22 nm peak) and BMV RNA (28 nm peak) are mixed simultaneously. Right, competition assays altering the order of addition of polyU and B1 (BMV RNA). (Reprinted with permission from Beren, Dreesens, Liu, Knobler, and Gelbart (2017)). (d) Free energy of encapsidation for linear and branched polynucleotides as a function of chain size. Left, effect of stiffness and charge density. Right, a closer look at the changes in charge density. Parameters are l (Kuhn length), τ (charge within one Kuhn segment), and f_b (fugacity). (Reprinted with permission from Li, Erdemci-Tandogan, van der Schoot, and Zandi (2018)). BMV, Brome mosaic virus; CP, capsid protein; VLP, virus-like particle

double for dsRNA, due to base-pairing. Accounting for these physical properties of RNA, Li and coworkers recently performed new calculations applying mean-field theory (Li, Erdemci-Tandogan, et al., 2018). The authors investigated the impact of RNA stiffness, by exploring changes in the mean Kuhn Length of the chains, and the effect of base-pairing on the distribution of the linear charge density. Interestingly, the effect of stiffness overshadows the charge density

contribution, when looking at free energy gains upon RNA encapsidation as a function of the polynucleotide size (Figure 4d). It also highlights the availability, within the free energy landscape, of certain conditions where the packaging of linear RNA becomes more favorable than for branched RNA (Figure 4d).

Thus, RNA base-pairing seems to have competing effects: (a) it makes RNA stiffer, increasing the work of packaging that must be overcome by the CPs; however, (b) it introduces branching junctions, hence, compactness, and (c) it enhances the charge density, both promoting efficient assembly. These results provide new insights into how linear ssRNA molecules can outcompete branched ones under assembly competition conditions. In addition, it is important to mention that these calculations are in full agreement with the already mentioned studies (Erdemci-Tandogan et al., 2014, 2016; Li et al., 2017; Perlmutter et al., 2013; Singaram et al., 2015), where the implications of RNA stiffness and charge density were not explored. Despite these new insights the models still predict that branched polymers have a competitive edge over linear ones, even when the effects of changes in stiffness and charge density are considered (Li, Erdemci-Tandogan, et al., 2018). This reveals that the existing theoretical frameworks do not yet capture essential aspects of assembly and clearly there is a need for both more (and maybe different) experiments as well as further developments in modeling/theory in order to understand how viral self-assembly occurs.

3 | MECHANICAL STABILITY OF VIRUSES

The material properties and mechanical stability of viruses are governed by several factors, such as for instance, (a) the inter- and intramolecular interactions (covalent, noncovalent, electrostatic, hydrophobic, etc.) of the capsid proteins (CPs; Ashcroft et al., 2005; Mateo, Diaz, Baranowski, & Mateu, 2003; Mateu, 2009, 2012, 2013; Reguera, Carreira, Riobobos, Almendral, & Mateu, 2004; Roos et al., 2012); (b) the protein(CP)-nucleic acid interactions (mostly electrostatic interactions at the capsid interior-nucleic acid interface; Devkota et al., 2009; Ni et al., 2012; Rao, 2006; Reade, Kakani, & Rochon, 2010; Schneemann, 2006; Snijder et al., 2013); (c) prestress resulting from capsid architecture or pressure associated with genome encapsidation (Baclayon et al., 2011; Carrasco et al., 2011; Klug, Roos, & Wuite, 2012; M. Marchetti, Wuite, & Roos, 2016); (d) stabilizing molecular interactions during assembly or maturation; for example, interaction with metal ions, scaffolding proteins, or enzymatic reactions, and so on (Li, Roy, Travesset, & Zandi, 2018; Perera & Kuhn, 2008; Persson, Tars, & Liljas, 2008; Plevka et al., 2009; P. E. Prevelige & Fane, 2012; Saugar et al., 2010); (e) entropic stabilization through capsid breathing and self-healing (C. Chen, Wang, & Zlotnick, 2011; de Pablo, Hernando-Perez, Carrasco, & Carrascosa, 2018; J. Lin et al., 2012; Reisdorph et al., 2003; Valbuena & Mateu, 2015). There is certainly overlap between these factors, and typically viruses are stabilized and sometimes also destabilized by a combination of them. This variety in properties influencing capsid stability makes its study a diverse field. The insights gained are not only useful for preventing or reducing viral infectivity, but also for the generation of artificial, hollow supramolecular assemblies (nanocages) for various uses in bio-nanotechnology, pharmacology, and materials sciences.

3.1 | AFM-based nanoindentation experiments

In order to characterize the mechanical properties of viruses and to capture particle-to-particle variations in these properties AFM-based force spectroscopy experiments have been developed (Ivanovska et al., 2004; Roos et al., 2010). A detailed experimental protocol of such AFM based nanoindentation experiments can be found in (Guo & Roos, 2019). Briefly, the viruses are first attached to a surface. It is important to have an attachment which is not so strong that the particle will be deformed, but it must not be too weak either so that it can roll over during the imaging/indentation. Next, the particle is localized by AFM imaging and a force distance curve (F-D) is taken on the center of the particle (Figure 5a). Another image of the particle is taken after the indentation to reveal the state of the particle after deformation. Typically, three different scenarios can be distinguished upon indentation. Depending on the viral mechanical architecture, the particle can exhibit a total collapse (Snijder, Uetrecht, et al., 2013; Figure 5b), or irreversible structural deformation whereby (a part of) the shell stays intact (Klug et al., 2012; Figure 5c), or self-recovery to its original size (de Pablo et al., 2018; Figure 5d). Upon analyzing the F-D curve one can deduce the stiffness of the particle (from the slope of the indentation curve), the ultimate strength of the particle (from the breaking force, if applicable), and the indentation depth (a mark of the deformability). In addition, using elasticity models one can also obtain an estimate for the intrinsic material properties in terms of Young's Modulus (Roos et al., 2010).

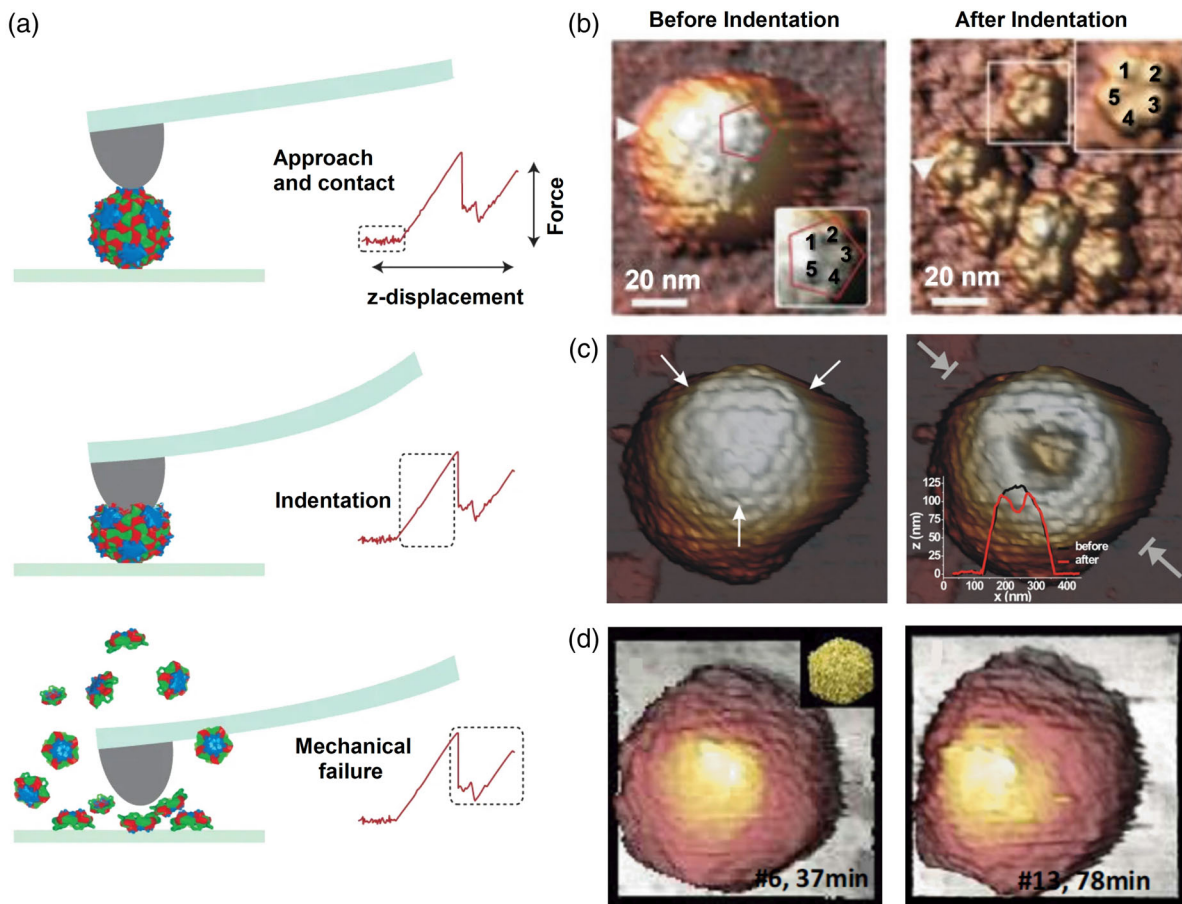


FIGURE 5 Response of virus particles to indentation forces. (a) Scheme of AFM nanoindentation experiment. (b–d) Examples of particles showing different effects upon indentation. (b) Mechanical failure of picorna-like *Triatoma* virus (TrV). (Panels adjusted from Snijder et al. (2013); with permission from the publisher). (c) Irreversible deformation of herpes simplex virus Type 1 (HSV1). (Panels adjusted from Klug et al. (2012); with permission from the publisher). (d) Reversible deformation of T7 bacteriophage. The particle shows plastic deformation immediate after the indentation, but resumed its structure after ~36 min (right panel). (Panels adapted from de Pablo et al. (2018); with permission from the publisher). AFM, atomic force microscopy

3.2 | Mechanical properties linked to viral assembly and disassembly

Initially, started as a curiosity driven quest (Ivanovska et al., 2004), nanoindentation-based mechanical studies of viruses is now a wider applied physical virology technique. The determination of mechanical properties of viruses is not only providing information about capsid stability, but also unveiling physicochemical and biological links between different stages in a virus-life cycle (Carrasco et al., 2006; Kol et al., 2007; Roos et al., 2010; Roos et al., 2012; Snijder, Utrecht, et al., 2013). For instance, Carrasco et al. (2011) have investigated the empty ϕ 29 bacteriophage proheads using AFM-based nanoindentation experiments in combination with coarse-grained simulations. In this work, a twofold anisotropic stiffening of the capsid along the short axis was observed. The authors concluded that during assembly curvature of the capsid protein is induced by the scaffolding proteins resulting in a structural stress within the proheads. This stress can then later be used as a trigger for DNA release through the tail region. Around the same time, Baclayon et al. (2011) have investigated Norwalk virus-like particles (NVLPs) to scrutinize the role of the protruding domain of the NVLP capsid protein in the particle's stability. It turned out that the presence of this domain generated a stabilizing prestress in the shell. This finding shows that the protruding domains are not only responsible for specific cell binding during the infection cycle, but also have a role in survival of the particle when exposed to stress factors.

Next to structural components in the capsid, also the internalized genome can influence disassembly. Nanoindentation of the picorna-like *Triatoma* virus was performed in combination with Mass Spectroscopy to

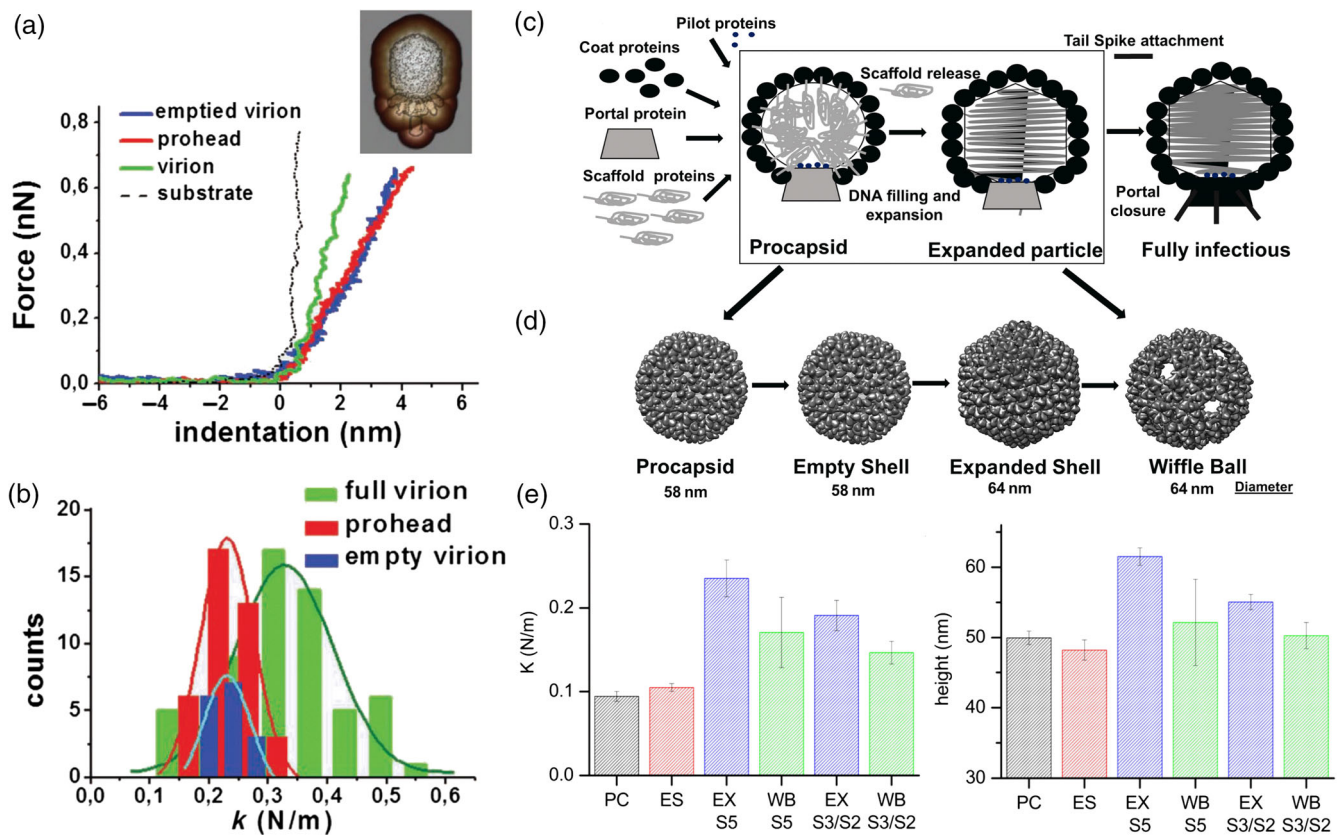


FIGURE 6 Effect of genome encapsulation and maturation. (a) Force-indentation curves obtained from an empty particle, a prohead and a complete virion of the ϕ 29 bacteriophage. Inset is a typical AFM image of a ϕ 29 bacteriophage virion, with a superimposed reconstruction from EM. (b) Calculated spring constant from the experiments in (a). (Panel a and b taken from Hernando-Perez et al. (2012), with permission from the publisher). (c) Scheme of in vivo maturation of bacteriophage P22. (d) P22 VLP reconstructions at different stages. (e) The measured spring constant (left) and height (right) of capsids in different stages. PC: procapsid, ES: empty capsid, EX: expanded shell for five-, three-, and twofold symmetry (S5, S3, and S2, respectively). (Panels taken from Kant et al. (2018); with permission from the publishers). AFM, atomic force microscopy

scrutinize its stability (Snijder, Utrecht, et al., 2013). Under the indentation force, the particle exhibited mechanical failure (Figure 5b). After particle disruption, AFM imaging revealed that the particle disassembled into its single penton structural units. While doing a pH sweep, it turned out that at neutral pH, the genome stabilizes the particle, but that at alkaline pH, it is destabilizing the capsid. This behavior seems to be linked to the infectious pathway in which the particle passes the alkaline parts of the gut before infection occurs. Genome induced stress also seems to play a role in human adenovirus (HAdV) disassembly (Ortega-Esteban et al., 2013; Ortega-Esteban et al., 2015). By continuous imaging of the particle with the AFM tip, at a certain moment fatigue occurred and the pentons started coming off the infectious particles. As these prolonged stresses are not likely to be the sole factor in disassembly during infection, other factors must facilitate this process. It turned out that binding of HAdV to the host cell receptor integrin $\alpha\beta$ 5 plays a pivotal role in the first stage of infection and particle destabilization (Snijder et al., 2013). By binding to integrin, a conformational change occurs in the penton base, thereby loosening it and facilitating the later release of the penton base. Minor capsid proteins, such as pUL17 and pUL25 of herpes simplex virus Type 1, can also influence particle stability (Snijder et al., 2017). Nanoindentation experiments with wild-type and deletion mutant particles revealed that these minor capsid proteins, which bind specifically close to the fivefold axis, bring stability to these weakest parts of the capsid. Finally, complex capsid structures such as the multilayered rotavirus turn out to have different mechanical properties for each layer, fitting with the needs for protection (stiff outer layer) and genome expression (flexible middle layer) at different stages of the life cycle (Jimenez-Zaragoza et al., 2018).

3.3 | Mechanical properties linked to genome encapsidation

As mentioned before, the encapsulation of genetic material can have a significant impact on capsid morphology and stability. Therefore, capturing the mechanical effects of the presence of the genome in viral shells is a way to gain insight into the physicochemical aspects of virus survival and infectivity. Nanoindentation experiments on MVM revealed anisotropic mechanical properties along the different symmetry axes in the DNA containing particles (Carrasco et al., 2006). Comparing with the response of empty capsids, it was concluded that the anisotropic reinforcement was mediated by DNA packaging. This interpretation was also supported by the crystal structure, in which short DNA patches at the inner capsid wall were visible. Combining with finite element modeling, the authors concluded that the MVM particle is not reinforced at their fivefold symmetric axis, in order to allow for DNA release during infection. In a follow-up study (Carrasco, Castellanos, de Pablo, & Mateu, 2008), specific mutation in the capsid protein were introduced to remove the DNA–capsid interaction. The measured change in material properties of the mutated particles, corroborated their earlier interpretations on the DNA mediated anisotropic reinforcement of the shell. As mentioned above, Triatoma virus shows an intricate interaction between capsid and genome with stabilizing interactions at neutral pH but destabilizing ones at higher pH (Snijder, Uetrecht, et al., 2013). This seems also directly related to disassembly. A change in stiffness upon genome encapsidation was furthermore observed for bacteriophage ϕ 29 (Hernando-Perez et al., 2012; Figure 6a,b). While the scaffolding protein did not play a significant role in the mechanical stability of the capsid, the presence of DNA resulted in a genome induced pressure of 40 ± 20 atm inside the virion. For SV40, genome encapsidation did not affect the stiffness, but it increased the particle resilience against large deformations (van Rosmalen, Li, Zlotnick, Wuite, & Roos, 2018). Furthermore, the VLP material properties were affected by the addition of the reducing agent DTT and calcium-ion chelating EDTA, with, respectively, a reduced resistance to mechanical stress and a softening of the shell as result. In a recent study on adenovirus stability (van Rosmalen, Nemerow, Wuite, & Roos, 2018), particles with a mutation in precursor protein VI were studied. It was revealed that the mutant exhibits a factor of two increase in stiffness, while the infectivity remains constant. The stiffening seems to be the result of the presence of pVII in the mature, mutant capsids, leading to DNA crosslinking. Interestingly, a study on HIV particles showed that sometimes not the genome itself (with or without crosslinking proteins), but reverse transcription of the genome is generating a pressure that leads to disassembly of the viral particle (Rankovic, Varadarajan, Ramalho, Aiken, & Rousso, 2017). Overall, it seems that there is a correlation between the Young's modulus and the manner of encapsidation of viruses. While viruses that self-assemble around their genome possess a relatively low Young's modulus, the modulus is higher for particles that self-assemble empty and that use a packaging motor to encapsidate the genome (Roos et al., 2010). The latter method is expected to lead to higher internal pressures and therefore the necessity for stronger shells to hold the pressurized genome.

3.4 | Mechanical properties linked to viral maturation

Capsids of viruses that undergo maturation typically go through a set of conformational changes. By studying the mechanical changes accompanying this process, insights are provided into these maturation steps. To scrutinize these steps in bacteriophage HK97, which is a λ -like phage, the particle was studied by AFM-based imaging and nanoindentation (Roos et al., 2012). It turned out that maturation results in an increase in mechanical stability of the capsid in three different ways: increasing Young's modulus of the mature capsid, increasing capsid strength, and increasing resistance to material fatigue. Phage λ undergoes maturation induced changes at the same positions in the capsid as phage HK97, but the changes in the latter are crosslinking of the capsid proteins and in the former an extra protein is added at those positions. It was shown that phage λ also increases its strength during maturation (Hernando-Perez, Lambert, Nakatani-Webster, Catalano, & de Pablo, 2014). So while these related phages have found completely unrelated ways of reinforcing their capsid during maturation, they both reinforce the same places in the capsid, indicating that these locations are the weak spots in the capsid. A comparative study of adenoviral maturation revealed that the genomic core of an immature particle shows a stiffer response than the mature core (Ortega-Esteban et al., 2015). The decondensation of the core upon maturation makes it more flexible and this flexibility is thought to facilitate genome release. This is, however, not the only factor in genome release, as first the pentons need to be removed from the capsid. The proteolytic cleavage of preprotein VI during maturation is essential for this penton destabilization, as revealed by imaging based fatigue experiments (Denning et al., 2019; Figure 7).

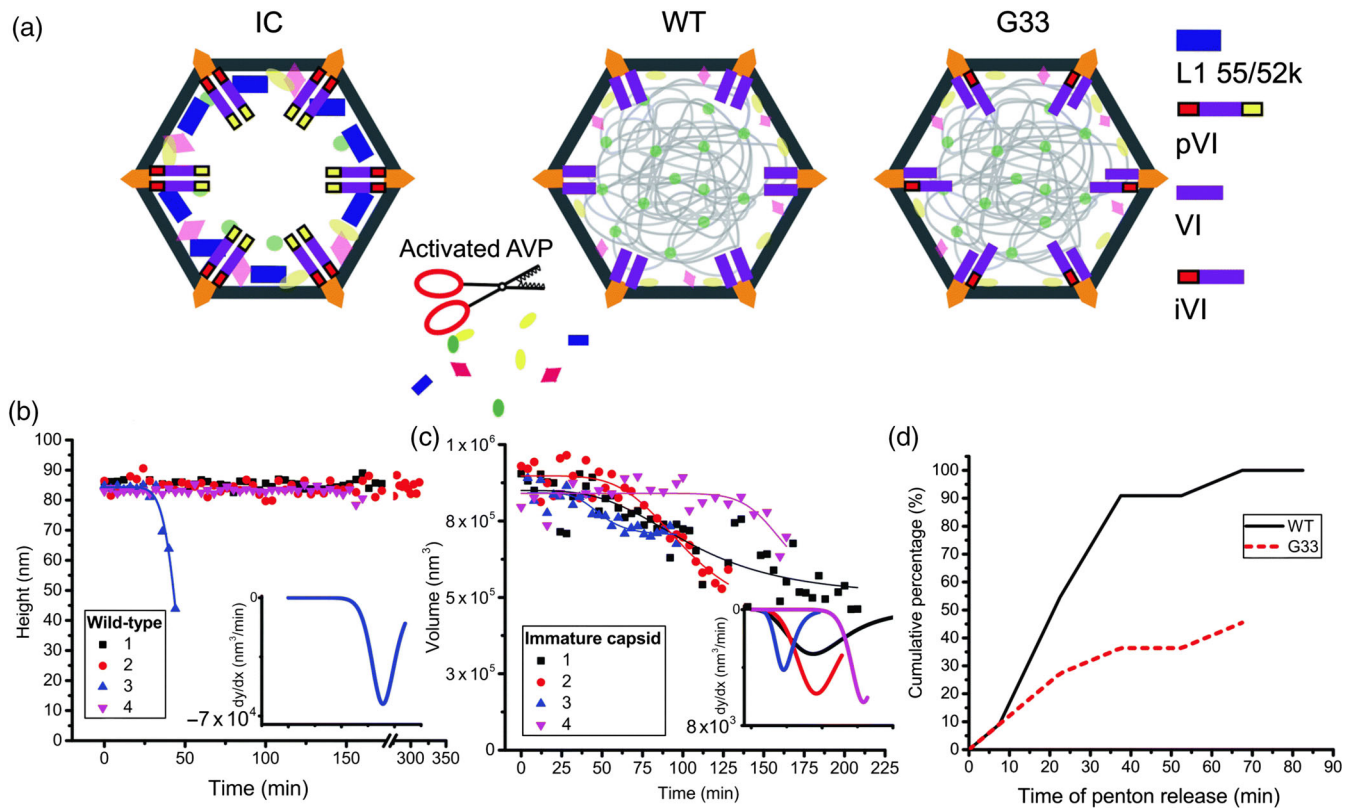


FIGURE 7 Mechanical fatigue of human adenovirus immature (IC), mature Ad5 (WT), and G33 mutant (G33) capsids. (a) Schematic representation of IC, WT, and G33 particles with relevant core component composition. (b) Plot of change in height over time for constant AFM imaging of WT particles. Inset: first derivative of sigmoidal fit from the plot in (b). (c) Plot of change in volume over imaging time for IC particles. Inset: first derivative of sigmoidal fit of curves in main panel. (d) Comparative representation of cumulative percentage of penton release of WT and G33 particles for AFM tip induced fatigue experiments. (Reproduced from Denning et al. (2019) with permission from The Royal Society of Chemistry). AFM, atomic force microscopy

While bacteriophage HK97 and λ undergo a stabilizing transition during maturation, it is the other way around for HIV. Immature HIV particles are more than 14-fold stiffer than mature particles, and this large difference is primarily mediated by the HIV envelope cytoplasmic tail domain (Kol et al., 2007). The authors showed that this stiffness switch is essential to inhibit immature particles to enter host cells. Bacteriophage P22 is known to undergo a series of intermediate stages during maturation (Parker & Prevelige Jr., 1998). While mimicking these intermediate stages, by application of thermal and chemical stresses, it was shown that the rigidity and brittleness increased after maturation induced expansion, as predicted by continuum elasticity theory (Kant et al., 2018; Figure 6c–e). For another bacteriophage, phage T7, it turned out that stiffness was not an ideal parameter to describe viral stability, but that the particle fragility provides a better characteristic (Hernando-Perez et al., 2014). This shows that various material properties can be used in order to elucidate the mechanics and stability of viral particles.

4 | CONCLUSION

Viruses possess extraordinary features and functions. They have evolved in close dependency to their living hosts, influencing the development of life. Therefore, the study of viral systems has impacts beyond virology. Viral systems present many *vital* characteristics found in living organisms. For instance, the capacity of viral components to self-assemble into supramolecular structures, to recognize specific targets, and to possess a high adaptability to environmental conditions. In addition, viruses are formed from selective biomacromolecules that exhibit the functions and specificity needed to hijack and dominate cellular processes. Recently, studies on viruses and their derived VLPs have grown drastically, not only to better understand viral and nonviral systems, but also due to the opportunities these systems have opened up in areas such as nanomedicine and (bio)nanotechnology. Here we have discussed how viral self-

assembly is relying on fine-tuned interactions between the capsid proteins and the viral genome. The balancing of these interactions, CP–CP and CP–genome, implicitly conditioned by the surrounding environment, will ultimately determine the assembly pathway(s). Certain viruses support specific packaging by including conserved genomic sequences that allow CPs to discriminate the cellular genetic material to ensure the formation of virions. Moreover, the PS-mediated assembly theory gives a comprehensive understanding for the successful formation of optimal capsid geometries within the conformational assembly landscape. However, other viruses seem to assemble showing residual or absence of sequence specificity, at least under in vitro conditions, where genome topology has proven to be a potential candidate to understand the assembly of these kind of viruses. Viruses and their derived VLPs are found within a broad range of material properties. Mechanics is not only an essential factor in genome encapsidation and maturation, but also in self-assembly and disassembly. In addition, viral systems have been proven to be highly dynamic, showing the capability to modulate stability during infection, which highlights their remarkable conformational plasticity and adaptability.

The discussed new insights in self-assembly and mechanics show how valuable physical virology approaches are. The single-particle methods and techniques presented here, such as AFM, EM, resistive-pulse sensing, and CDMS; in combination with bulk methods, simulations, and theoretical calculations, have proven to be a good combination of approaches to shed light onto the molecular basis of viral systems. Still a lot of open questions remain, and there is an urgent need for innovative methods in order to finally elucidate the mechanisms behind assembly. In this respect, novel approaches such as magnetic tweezers, optical tweezers, acoustic force spectroscopy, and high-speed AFM, which present advances in temporal and spatial resolution, seem promising techniques to follow viral assembly in real time, and at the single-particle level. A very recent example of this is assembly studies by optical tweezers (K. D. Marchetti et al., 2019). With these new techniques and approaches, it is expected that in the coming years our understanding of viral self-assembly and mechanics will be further deepened. The hereby newly generated insights will likely not only advance fundamental science, but also applications of viruses and VLPs.

ACKNOWLEDGMENTS

W.H.R. acknowledges support from the Nederlandse organisatie voor Wetenschappelijk Onderzoek (NWO) through a Vidi grant and a STW Perspectief programme. S.M. thanks the EU for a Marie Curie grant.

CONFLICT OF INTEREST

The authors have declared no conflicts of interest for this article.

AUTHOR CONTRIBUTIONS

Pedro Buzón: Writing-original draft and writing-review and editing-Equal. **Sourav Maity:** Writing-original draft and writing-review and editing. **Wouter Roos:** Conceptualization; supervision; writing-original draft; and writing-review and editing.

ORCID

Pedro Buzón  <https://orcid.org/0000-0002-1282-9006>

Wouter H. Roos  <https://orcid.org/0000-0002-5104-0139>

RELATED WIREs ARTICLES

[Synthetic virology: Engineering viruses for gene delivery](#)

[Viral chemistry: The chemical functionalization of viral architectures to create new technology](#)

[Synthetic plant virology for nanobiotechnology and nanomedicine](#)

[Physical, chemical, and synthetic virology: Reprogramming viruses as controllable nanodevices](#)

REFERENCES

- Abels, J. A., Moreno-Herrero, F., van der Heijden, T., Dekker, C., & Dekker, N. H. (2005). Single-molecule measurements of the persistence length of double-stranded RNA. *Biophysical Journal*, *88*(4), 2737–2744. <https://doi.org/10.1529/biophysj.104.052811>
- Ashcroft, A. E., Lago, H., Macedo, J. M., Horn, W. T., Stonehouse, N. J., & Stockley, P. G. (2005). Engineering thermal stability in RNA phage capsids via disulphide bonds. *Journal of Nanoscience and Nanotechnology*, *5*(12), 2034–2041.
- Baclayon, M., Shoemaker, G. K., Uetrecht, C., Crawford, S. E., Estes, M. K., Prasad, B. V., ... Roos, W. H. (2011). Prestress strengthens the shell of Norwalk virus nanoparticles. *Nano Letters*, *11*(11), 4865–4869. <https://doi.org/10.1021/nl202699r>

- Bancroft, J. B., & Hiebert, E. (1967). Formation of an infectious nucleoprotein from protein and nucleic acid isolated from a small spherical virus. *Virology*, *32*(2), 354–356. [https://doi.org/10.1016/0042-6822\(67\)90284-X](https://doi.org/10.1016/0042-6822(67)90284-X)
- Bancroft, J. B., Hiebert, E., & Bracker, C. E. (1969). The effects of various polyanions on shell formation of some spherical viruses. *Virology*, *39*(4), 924–930. [https://doi.org/10.1016/0042-6822\(69\)90029-4](https://doi.org/10.1016/0042-6822(69)90029-4)
- Ben-Shaul, A., & Gelbart, W. M. (2015). Viral ssRNAs are indeed compact. *Biophysical Journal*, *108*(1), 14–16. <https://doi.org/10.1016/j.bpj.2014.11.010>
- Beren, C., Dreesens, L. L., Liu, K. N., Knobler, C. M., & Gelbart, W. M. (2017). The effect of RNA secondary structure on the self-assembly of viral capsids. *Biophysical Journal*, *113*(2), 339–347. <https://doi.org/10.1016/j.bpj.2017.06.038>
- Bernal, J. D. (1959). The scale of structural units in biopoiesis. In A. I. Oparin, A. E. Braunshtein, A. G. Pasynskiĭ, & T. E. Pavlovskaya (Eds.), *The origin of life on the earth* (pp. 385–399). Oxford, England: Pergamon.
- Bhella, D. (2018). Virus proteins and nucleoproteins: An overview. *Sub-Cellular Biochemistry*, *88*, 1–18. https://doi.org/10.1007/978-981-10-8456-0_1
- Bruinsma, R. F., Comas-Garcia, M., Garmann, R. F., & Grosberg, A. Y. (2016). Equilibrium self-assembly of small RNA viruses. *Physical Review E*, *93*(3), 032405. <https://doi.org/10.1103/PhysRevE.93.032405>
- Butterfield, G. L., Lajoie, M. J., Gustafson, H. H., Sellers, D. L., Nattermann, U., Ellis, D., ... Baker, D. (2017). Evolution of a designed protein assembly encapsulating its own RNA genome. *Nature*, *552*(7685), 415–420. <https://doi.org/10.1038/nature25157>
- Carrasco, C., Carreira, A., Schaap, I. A., Serena, P. A., Gomez-Herrero, J., Mateu, M. G., & de Pablo, P. J. (2006). DNA-mediated anisotropic mechanical reinforcement of a virus. *Proceedings of the National Academy of Sciences of the United States of America*, *103*(37), 13706–13711. <https://doi.org/10.1073/pnas.0601881103>
- Carrasco, C., Castellanos, M., de Pablo, P. J., & Mateu, M. G. (2008). Manipulation of the mechanical properties of a virus by protein engineering. *Proceedings of the National Academy of Sciences of the United States of America*, *105*(11), 4150–4155. <https://doi.org/10.1073/pnas.0708017105>
- Carrasco, C., Luque, A., Hernando-Perez, M., Miranda, R., Carrascosa, J. L., Serena, P. A., ... de Pablo, P. J. (2011). Built-in mechanical stress in viral shells. *Biophysical Journal*, *100*(4), 1100–1108. <https://doi.org/10.1016/j.bpj.2011.01.008>
- Caspar, D. L. D., & Klug, A. (1962). Physical principles in the construction of regular viruses. *Cold Spring Harbor Symposia on Quantitative Biology*, *27*, 1–24. <https://doi.org/10.1101/sqb.1962.027.001.005>
- Ceres, P., & Zlotnick, A. (2002). Weak protein-protein interactions are sufficient to drive assembly of hepatitis B virus capsids. *Biochemistry*, *41*(39), 11525–11531.
- Comas-Garcia, M. (2019). Packaging of genomic RNA in positive-sense single-stranded RNA viruses: A complex story. *Viruses*, *11*(3), 1–23. <https://doi.org/10.3390/v11030253>
- Comas-Garcia, M., Cadena-Nava, R. D., Rao, A. L., Knobler, C. M., & Gelbart, W. M. (2012). In vitro quantification of the relative packaging efficiencies of single-stranded RNA molecules by viral capsid protein. *Journal of Virology*, *86*(22), 12271–12282. <https://doi.org/10.1128/JVI.01695-12>
- Comas-Garcia, M., Datta, S. A., Baker, L., Varma, R., Gudla, P. R., & Rein, A. (2017). Dissection of specific binding of HIV-1 Gag to the ‘packaging signal’ in viral RNA. *eLife*, *6*, 1–27. <https://doi.org/10.7554/eLife.27055>
- Comas-Garcia, M., Davis, S. R., & Rein, A. (2016). On the selective packaging of genomic RNA by HIV-1. *Viruses*, *8*(9), 1–12. <https://doi.org/10.3390/v8090246>
- Comas-Garcia, M., Kroupa, T., Datta, S. A., Harvin, D. P., Hu, W. S., & Rein, A. (2018). Efficient support of virus-like particle assembly by the HIV-1 packaging signal. *eLife*, *7*, 1–11. <https://doi.org/10.7554/eLife.38438>
- Cordova, A., Deserno, M., Gelbart, W. M., & Ben-Shaul, A. (2003). Osmotic shock and the strength of viral capsids. *Biophysical Journal*, *85*(1), 70–74. [https://doi.org/10.1016/S0006-3495\(03\)74455-5](https://doi.org/10.1016/S0006-3495(03)74455-5)
- Crick, F. H., & Watson, J. D. (1956). Structure of small viruses. *Nature*, *177*(4506), 473–475. <https://doi.org/10.1038/177473a0>
- Crowther, R. A., Kiselev, N. A., Bottcher, B., Berriman, J. A., Borisova, G. P., Ose, V., & Pumpens, P. (1994). Three-dimensional structure of hepatitis B virus core particles determined by electron cryomicroscopy. *Cell*, *77*(6), 943–950.
- Cuervo, A., Dauden, M. I., & Carrascosa, J. L. (2013). Nucleic acid packaging in viruses. *Sub-Cellular Biochemistry*, *68*, 361–394. https://doi.org/10.1007/978-94-007-6552-8_12
- Chen, C., Wang, J. C., & Zlotnick, A. (2011). A kinase chaperones hepatitis B virus capsid assembly and captures capsid dynamics in vitro. *PLoS Pathogens*, *7*(11), e1002388. <https://doi.org/10.1371/journal.ppat.1002388>
- Chen, H., Meisburger, S. P., Pabit, S. A., Sutton, J. L., Webb, W. W., & Pollack, L. (2012). Ionic strength-dependent persistence lengths of single-stranded RNA and DNA. *Proceedings of the National Academy of Sciences of the United States of America*, *109*(3), 799–804. <https://doi.org/10.1073/pnas.1119057109>
- Chevreuil, M., Law-Hine, D., Chen, J., Bressanelli, S., Combet, S., Constantin, D., ... Tresset, G. (2018). Nonequilibrium self-assembly dynamics of icosahedral viral capsids packaging genome or polyelectrolyte. *Nature Communications*, *9*(1), 3071. <https://doi.org/10.1038/s41467-018-05426-8>
- Dai, X., Li, Z., Lai, M., Shu, S., Du, Y., Zhou, Z. H., & Sun, R. (2017). In situ structures of the genome and genome-delivery apparatus in a single-stranded RNA virus. *Nature*, *541*(7635), 112–116. <https://doi.org/10.1038/nature20589>
- de Pablo, P. J. (2018). Atomic force microscopy of virus shells. *Seminars in Cell & Developmental Biology*, *73*, 199–208. <https://doi.org/10.1016/j.semcdb.2017.08.039>

- de Pablo, P. J., Hernando-Perez, M., Carrasco, C., & Carrascosa, J. L. (2018). Direct visualization of single virus restoration after damage in real time. *Journal of Biological Physics*, *44*(2), 225–235. <https://doi.org/10.1007/s10867-018-9492-9>
- del Alamo, M., & Mateu, M. G. (2005). Electrostatic repulsion, compensatory mutations, and long-range non-additive effects at the dimerization interface of the HIV capsid protein. *Journal of Molecular Biology*, *345*(4), 893–906. <https://doi.org/10.1016/j.jmb.2004.10.086>
- Denning, D., Bennett, S., Mullen, T., Moyer, C., Vorselen, D., Wuite, G. J. L., ... Roos, W. H. (2019). Maturation of adenovirus primes the protein nano-shell for successful endosomal escape. *Nanoscale*, *11*(9), 4015–4024. <https://doi.org/10.1039/c8nr10182e>
- Devkota, B., Petrov, A. S., Lemieux, S., Boz, M. B., Tang, L., Schneemann, A., ... Harvey, S. C. (2009). Structural and electrostatic characterization of pariacoto virus: Implications for viral assembly. *Biopolymers*, *91*(7), 530–538. <https://doi.org/10.1002/bip.21168>
- Dykeman, E. C., Stockley, P. G., & Twarock, R. (2013a). Building a viral capsid in the presence of genomic RNA. *Physical Review E*, *87*(2), 022717. <https://doi.org/10.1103/PhysRevE.87.022717>
- Dykeman, E. C., Stockley, P. G., & Twarock, R. (2013b). Packaging signals in two single-stranded RNA viruses imply a conserved assembly mechanism and geometry of the packaged genome. *Journal of Molecular Biology*, *425*(17), 3235–3249. <https://doi.org/10.1016/j.jmb.2013.06.005>
- Dykeman, E. C., Stockley, P. G., & Twarock, R. (2014). Solving a Levinthal's paradox for virus assembly identifies a unique antiviral strategy. *Proceedings of the National Academy of Sciences of the United States of America*, *111*(14), 5361–5366. <https://doi.org/10.1073/pnas.1319479111>
- Eber, F. J., Eiben, S., Jeske, H., & Wege, C. (2015). RNA-controlled assembly of tobacco mosaic virus-derived complex structures: From nanoboomerangs to tetrapods. *Nanoscale*, *7*(1), 344–355. <https://doi.org/10.1039/c4nr05434b>
- Eigen, M. (2000). Viruses: evolution, propagation, and defense. *Nutrition Reviews*, *58*(2 Pt 2), S5–S16.
- Elrad, O. M., & Hagan, M. F. (2010). Encapsulation of a polymer by an icosahedral virus. *Physical Biology*, *7*(4), 045003. <https://doi.org/10.1088/1478-3975/7/4/045003>
- Endres, D., & Zlotnick, A. (2002). Model-based analysis of assembly kinetics for virus capsids or other spherical polymers. *Biophysical Journal*, *83*(2), 1217–1230. [https://doi.org/10.1016/S0006-3495\(02\)75245-4](https://doi.org/10.1016/S0006-3495(02)75245-4)
- Erdemci-Tandogan, G., Wagner, J., van der Schoot, P., Podgornik, R., & Zandi, R. (2014). RNA topology remodels electrostatic stabilization of viruses. *Physical Review E*, *89*(3), 032707. <https://doi.org/10.1103/PhysRevE.89.032707>
- Erdemci-Tandogan, G., Wagner, J., van der Schoot, P., Podgornik, R., & Zandi, R. (2016). Effects of RNA branching on the electrostatic stabilization of viruses. *Physical Review E*, *94*(2–1), 022408. <https://doi.org/10.1103/PhysRevE.94.022408>
- Fernandez de Castro, I., Tenorio, R., & Risco, C. (2016). Virus assembly factories in a lipid world. *Current Opinion in Virology*, *18*, 20–26. <https://doi.org/10.1016/j.coviro.2016.02.009>
- Fraenkel-Conrat, H., & Williams, R. C. (1955). Reconstitution of active tobacco mosaic virus from its inactive protein and nucleic acid components. *Proceedings of the National Academy of Sciences of the United States of America*, *41*(10), 690–698.
- Garmann, R. F., Comas-Garcia, M., Knobler, C. M., & Gelbart, W. M. (2016). Physical principles in the self-assembly of a simple spherical virus. *Accounts of Chemical Research*, *49*(1), 48–55. <https://doi.org/10.1021/acs.accounts.5b00350>
- Gopal, A., Zhou, Z. H., Knobler, C. M., & Gelbart, W. M. (2012). Visualizing large RNA molecules in solution. *RNA*, *18*(2), 284–299. <https://doi.org/10.1261/rna.027557.111>
- Guo, Y., & Roos, W. H. (2019). AFM nanoindentation experiments on protein shells: A protocol. *Methods in Molecular Biology*, *1886*, 243–257. https://doi.org/10.1007/978-1-4939-8894-5_14
- Hagan, M. F. (2014). Modeling viral capsid assembly. *Advances in Chemical Physics*, *155*, 1–68. <https://doi.org/10.1002/9781118755815.ch01>
- Hagan, M. F., & Elrad, O. M. (2010). Understanding the concentration dependence of viral capsid assembly kinetics—The origin of the lag time and identifying the critical nucleus size. *Biophysical Journal*, *98*(6), 1065–1074. <https://doi.org/10.1016/j.bpj.2009.11.023>
- Hernandez-Garcia, A., Kraft, D. J., Janssen, A. F., Bomans, P. H., Sommerdijk, N. A., Thies-Weesie, D. M., ... de Vries, R. (2014). Design and self-assembly of simple coat proteins for artificial viruses. *Nature Nanotechnology*, *9*(9), 698–702. <https://doi.org/10.1038/nnano.2014.169>
- Hernando-Perez, M., Lambert, S., Nakatani-Webster, E., Catalano, C. E., & de Pablo, P. J. (2014). Cementing proteins provide extra mechanical stabilization to viral cages. *Nature Communications*, *5*, 4520. <https://doi.org/10.1038/ncomms5520>
- Hernando-Perez, M., Miranda, R., Aznar, M., Carrascosa, J. L., Schaap, I. A., Reguera, D., & de Pablo, P. J. (2012). Direct measurement of phage phi29 stiffness provides evidence of internal pressure. *Small*, *8*(15), 2366–2370. <https://doi.org/10.1002/sml.201200664>
- Hernando-Perez, M., Pascual, E., Aznar, M., Ionel, A., Caston, J. R., Luque, A., ... de Pablo, P. J. (2014). The interplay between mechanics and stability of viral cages. *Nanoscale*, *6*(5), 2702–2709. <https://doi.org/10.1039/c3nr05763a>
- Hohn, T. (1969). Role of RNA in the assembly process of bacteriophage ϕ r. *Journal of Molecular Biology*, *43*(1), 191–200.
- Ivanovska, I. L., de Pablo, P. J., Ibarra, B., Sgalari, G., MacKintosh, F. C., Carrascosa, J. L., ... Wuite, G. J. (2004). Bacteriophage capsids: Tough nanoshells with complex elastic properties. *Proceedings of the National Academy of Sciences of the United States of America*, *101*(20), 7600–7605. <https://doi.org/10.1073/pnas.0308198101>
- Jimenez-Zaragoza, M., Yubero, M. P., Martin-Forero, E., Caston, J. R., Reguera, D., Luque, D., ... Rodriguez, J. M. (2018). Biophysical properties of single rotavirus particles account for the functions of protein shells in a multilayered virus. *eLife*, *7*, 1–23. <https://doi.org/10.7554/eLife.37295>
- Kant, R., Llauro, A., Rayaprolu, V., Qazi, S., de Pablo, P. J., Douglas, T., & Bothner, B. (2018). Changes in the stability and biomechanics of P22 bacteriophage capsid during maturation. *Biochimica et Biophysica Acta: General Subjects*, *1862*(6), 1492–1504. <https://doi.org/10.1016/j.bbagen.2018.03.006>
- Kebbekus, P., Draper, D. E., & Hagerman, P. (1995). Persistence length of RNA. *Biochemistry*, *34*(13), 4354–4357. <https://doi.org/10.1021/bi00013a026>

- Kegel, W. K., & van der Schoot, P. (2006). Physical regulation of the self-assembly of tobacco mosaic virus coat protein. *Biophysical Journal*, 91(4), 1501–1512. <https://doi.org/10.1529/biophysj.105.072603>
- King, N. P., Sheffler, W., Sawaya, M. R., Vollmar, B. S., Sumida, J. P., Andre, I., ... Baker, D. (2012). Computational design of self-assembling protein nanomaterials with atomic level accuracy. *Science*, 336(6085), 1171–1174. <https://doi.org/10.1126/science.1219364>
- Klug, W. S., Roos, W. H., & Wuite, G. J. (2012). Unlocking internal prestress from protein nanoshells. *Physical Review Letters*, 109(16), 168104. <https://doi.org/10.1103/PhysRevLett.109.168104>
- Kol, N., Shi, Y., Tsvitov, M., Barlam, D., Shneck, R. Z., Kay, M. S., & Rousso, I. (2007). A stiffness switch in human immunodeficiency virus. *Biophysical Journal*, 92(5), 1777–1783. <https://doi.org/10.1529/biophysj.106.093914>
- Koning, R. I., Gomez-Blanco, J., Akopjana, I., Vargas, J., Kazaks, A., Tars, K., ... Koster, A. J. (2016). Asymmetric cryo-EM reconstruction of phage MS2 reveals genome structure in situ. *Nature Communications*, 7, 12524. <https://doi.org/10.1038/ncomms12524>
- Lam, P., & Steinmetz, N. F. (2018). Plant viral and bacteriophage delivery of nucleic acid therapeutics. *WIREs Nanomedicine and Nanobiotechnology*, 10(1), 1–18. <https://doi.org/10.1002/wnan.1487>
- Lee, L. S., Brunk, N., Haywood, D. G., Keifer, D., Pierson, E., Kondylis, P., ... Zlotnick, A. (2017). A molecular breadboard: Removal and replacement of subunits in a hepatitis B virus capsid. *Protein Science*, 26(11), 2170–2180. <https://doi.org/10.1002/pro.3265>
- Li, S., Erdemci-Tandogan, G., van der Schoot, P., & Zandi, R. (2018). The effect of RNA stiffness on the self-assembly of virus particles. *Journal of Physics: Condensed Matter*, 30(4), 044002. <https://doi.org/10.1088/1361-648X/aaa159>
- Li, S., Erdemci-Tandogan, G., Wagner, J., van der Schoot, P., & Zandi, R. (2017). Impact of a nonuniform charge distribution on virus assembly. *Physical Review E*, 96(2–1), 022401. <https://doi.org/10.1103/PhysRevE.96.022401>
- Li, S., Roy, P., Travesset, A., & Zandi, R. (2018). Why large icosahedral viruses need scaffolding proteins. *Proceedings of the National Academy of Sciences of the United States of America*, 115(43), 10971–10976. <https://doi.org/10.1073/pnas.1807706115>
- Lin, H. K., van der Schoot, P., & Zandi, R. (2012). Impact of charge variation on the encapsulation of nanoparticles by virus coat proteins. *Physical Biology*, 9(6), 066004. <https://doi.org/10.1088/1478-3975/9/6/066004>
- Lin, J., Lee, L. Y., Roivainen, M., Filman, D. J., Hogle, J. M., & Belnap, D. M. (2012). Structure of the Fab-labeled “breathing” state of native poliovirus. *Journal of Virology*, 86(10), 5959–5962. <https://doi.org/10.1128/JVI.05990-11>
- Lutomski, C. A., Lykтей, N. A., Pierson, E. E., Zhao, Z., Zlotnick, A., & Jarrold, M. F. (2018). Multiple pathways in capsid assembly. *Journal of the American Chemical Society*, 140(17), 5784–5790. <https://doi.org/10.1021/jacs.8b01804>
- Lutomski, C. A., Lykтей, N. A., Zhao, Z., Pierson, E. E., Zlotnick, A., & Jarrold, M. F. (2017). Hepatitis B virus capsid completion occurs through error correction. *Journal of the American Chemical Society*, 139(46), 16932–16938. <https://doi.org/10.1021/jacs.7b09932>
- Marchetti Kamsma, D., Cazares Vargas, E., Hernandez García, A., van der Schoot, P., de Vries, R., ... Roos, W. H. (2019). Real-time assembly of viruslike nucleocapsids elucidated at the single-particle level. *Nano Letters*, 19(8), 5746–5753. <https://doi.org/10.1021/acs.nanolett.9b02376>
- Marchetti, M., Wuite, G., & Roos, W. H. (2016). Atomic force microscopy observation and characterization of single virions and virus-like particles by nano-indentation. *Current Opinion in Virology*, 18, 82–88. <https://doi.org/10.1016/j.coviro.2016.05.002>
- Mateo, R., Diaz, A., Baranowski, E., & Mateu, M. G. (2003). Complete alanine scanning of intersubunit interfaces in a foot-and-mouth disease virus capsid reveals critical contributions of many side chains to particle stability and viral function. *The Journal of Biological Chemistry*, 278(42), 41019–41027. <https://doi.org/10.1074/jbc.M304990200>
- Mateu, M. G. (2009). The capsid protein of human immunodeficiency virus: Intersubunit interactions during virus assembly. *The FEBS Journal*, 276(21), 6098–6109. <https://doi.org/10.1111/j.1742-4658.2009.07313.x>
- Mateu, M. G. (2012). Mechanical properties of viruses analyzed by atomic force microscopy: A virological perspective. *Virus Research*, 168(1–2), 1–22. <https://doi.org/10.1016/j.virusres.2012.06.008>
- Mateu, M. G. (2013). Assembly, stability and dynamics of virus capsids. *Archives of Biochemistry and Biophysics*, 531(1–2), 65–79. <https://doi.org/10.1016/j.abb.2012.10.015>
- Medrano, M., Fuertes, M. A., Valbuena, A., Carrillo, P. J., Rodriguez-Huete, A., & Mateu, M. G. (2016). Imaging and quantitation of a succession of transient intermediates reveal the reversible self-assembly pathway of a simple icosahedral virus capsid. *Journal of the American Chemical Society*, 138(47), 15385–15396. <https://doi.org/10.1021/jacs.6b07663>
- Michaels, T. C. T., Bellaiche, M. M. J., Hagan, M. F., & Knowles, T. P. J. (2017). Kinetic constraints on self-assembly into closed supramolecular structures. *Scientific Reports*, 7(1), 12295. <https://doi.org/10.1038/s41598-017-12528-8>
- Milo, R. (2013). What is the total number of protein molecules per cell volume? A call to rethink some published values. *BioEssays: News and Reviews in Molecular, Cellular and Developmental Biology*, 35(12), 1050–1055. <https://doi.org/10.1002/bies.201300066>
- Nair, S., Li, L., Francis, S., Turner, W. W., VanNieuwenhze, M., & Zlotnick, A. (2018). Use of a fluorescent analogue of a HBV Core protein-directed drug to interrogate an antiviral mechanism. *Journal of the American Chemical Society*, 140(45), 15261–15269. <https://doi.org/10.1021/jacs.8b07988>
- Nguyen, H. D., Reddy, V. S., & Brooks, C. L., 3rd. (2007). Deciphering the kinetic mechanism of spontaneous self-assembly of icosahedral capsids. *Nano Letters*, 7(2), 338–344. <https://doi.org/10.1021/nl062449h>
- Ni, P., Wang, Z., Ma, X., Das, N. C., Sokol, P., Chiu, W., ... Kao, C. C. (2012). An examination of the electrostatic interactions between the N-terminal tail of the brome mosaic virus coat protein and encapsidated RNAs. *Journal of Molecular Biology*, 419(5), 284–300. <https://doi.org/10.1016/j.jmb.2012.03.023>
- Ortega-Esteban, A., Condezo, G. N., Perez-Berna, A. J., Chillon, M., Flint, S. J., Reguera, D., ... de Pablo, P. J. (2015). Mechanics of viral chromatin reveals the pressurization of human adenovirus. *ACS Nano*, 9(11), 10826–10833. <https://doi.org/10.1021/acsnano.5b03417>

- Ortega-Esteban, A., Perez-Berna, A. J., Menendez-Conejero, R., Flint, S. J., San Martin, C., & de Pablo, P. J. (2013). Monitoring dynamics of human adenovirus disassembly induced by mechanical fatigue. *Scientific Reports*, 3, 1434. <https://doi.org/10.1038/srep01434>
- Parker, M. H., & Prevelige, P. E., Jr. (1998). Electrostatic interactions drive scaffolding/coat protein binding and procapsid maturation in bacteriophage P22. *Virology*, 250(2), 337–349. <https://doi.org/10.1006/viro.1998.9386>
- Patel, N., Dykeman, E. C., Coutts, R. H., Lomonosoff, G. P., Rowlands, D. J., Phillips, S. E., ... Stockley, P. G. (2015). Revealing the density of encoded functions in a viral RNA. *Proceedings of the National Academy of Sciences of the United States of America*, 112(7), 2227–2232. <https://doi.org/10.1073/pnas.1420812112>
- Patel, N., White, S. J., Thompson, R. F., Bingham, R., Weiß, E. U., Maskell, D. P., ... Stockley, P. G. (2017). HBV RNA pre-genome encodes specific motifs that mediate interactions with the viral core protein that promote nucleocapsid assembly. *Nature Microbiology*, 2, 17098. <https://doi.org/10.1038/nmicrobiol.2017.98>
- Patel, N., Wroblewski, E., Leonov, G., Phillips, S. E. V., Tuma, R., Twarock, R., & Stockley, P. G. (2017). Rewriting nature's assembly manual for a ssRNA virus. *Proceedings of the National Academy of Sciences of the United States of America*, 114(46), 12255–12260. <https://doi.org/10.1073/pnas.1706951114>
- Perera, R., & Kuhn, R. J. (2008). Structural proteomics of dengue virus. *Current Opinion in Microbiology*, 11(4), 369–377. <https://doi.org/10.1016/j.mib.2008.06.004>
- Perlmutter, J. D., & Hagan, M. F. (2015a). Mechanisms of virus assembly. *Annual Review of Physical Chemistry*, 66, 217–239. <https://doi.org/10.1146/annurev-physchem-040214-121637>
- Perlmutter, J. D., & Hagan, M. F. (2015b). The role of packaging sites in efficient and specific virus assembly. *Journal of Molecular Biology*, 427(15), 2451–2467. <https://doi.org/10.1016/j.jmb.2015.05.008>
- Perlmutter, J. D., Perkett, M. R., & Hagan, M. F. (2014). Pathways for virus assembly around nucleic acids. *Journal of Molecular Biology*, 426(18), 3148–3165. <https://doi.org/10.1016/j.jmb.2014.07.004>
- Perlmutter, J. D., Qiao, C., & Hagan, M. F. (2013). Viral genome structures are optimal for capsid assembly. *eLife*, 2, e00632. <https://doi.org/10.7554/eLife.00632>
- Persson, M., Tars, K., & Liljas, L. (2008). The capsid of the small RNA phage PRR1 is stabilized by metal ions. *Journal of Molecular Biology*, 383(4), 914–922. <https://doi.org/10.1016/j.jmb.2008.08.060>
- Plevka, P., Kazaks, A., Voronkova, T., Kotelovica, S., Dishlers, A., Liljas, L., & Tars, K. (2009). The structure of bacteriophage phiCb5 reveals a role of the RNA genome and metal ions in particle stability and assembly. *Journal of Molecular Biology*, 391(3), 635–647. <https://doi.org/10.1016/j.jmb.2009.06.047>
- Porterfield, J. Z., Dhason, M. S., Loeb, D. D., Nassal, M., Stray, S. J., & Zlotnick, A. (2010). Full-length hepatitis B virus core protein packages viral and heterologous RNA with similarly high levels of cooperativity. *Journal of Virology*, 84(14), 7174–7184. <https://doi.org/10.1128/JVI.00586-10>
- Prevelige, P. E., & Fane, B. A. (2012). Building the machines: Scaffolding protein functions during bacteriophage morphogenesis. *Advances in Experimental Medicine and Biology*, 726, 325–350. https://doi.org/10.1007/978-1-4614-0980-9_14
- Prevelige, P. E., Jr., Thomas, D., & King, J. (1993). Nucleation and growth phases in the polymerization of coat and scaffolding subunits into icosahedral procapsid shells. *Biophysical Journal*, 64(3), 824–835. [https://doi.org/10.1016/S0006-3495\(93\)81443-7](https://doi.org/10.1016/S0006-3495(93)81443-7)
- Rankovic, S., Varadarajan, J., Ramalho, R., Aiken, C., & Rousso, I. (2017). Reverse transcription mechanically initiates HIV-1 capsid disassembly. *Journal of Virology*, 91(12), 1–14. <https://doi.org/10.1128/JVI.00289-17>
- Rao, A. L. (2006). Genome packaging by spherical plant RNA viruses. *Annual Review of Phytopathology*, 44, 61–87. <https://doi.org/10.1146/annurev.phyto.44.070505.143334>
- Reade, R., Kakani, K., & Rochon, D. (2010). A highly basic KGKKGK sequence in the RNA-binding domain of the cucumber necrosis virus coat protein is associated with encapsidation of full-length CNV RNA during infection. *Virology*, 403(2), 181–188. <https://doi.org/10.1016/j.virol.2010.03.045>
- Reguera, J., Carreira, A., Riobobos, L., Almendral, J. M., & Mateu, M. G. (2004). Role of interfacial amino acid residues in assembly, stability, and conformation of a spherical virus capsid. *Proceedings of the National Academy of Sciences of the United States of America*, 101(9), 2724–2729. <https://doi.org/10.1073/pnas.0307748101>
- Reisdorph, N., Thomas, J. J., Katpally, U., Chase, E., Harris, K., Siuzdak, G., & Smith, T. J. (2003). Human rhinovirus capsid dynamics is controlled by canyon flexibility. *Virology*, 314(1), 34–44.
- Rolfsson, O., Middleton, S., Manfield, I. W., White, S. J., Fan, B., Vaughan, R., ... Stockley, P. G. (2016). Direct evidence for packaging signal-mediated assembly of bacteriophage MS2. *Journal of Molecular Biology*, 428(2 Pt B), 431–448. <https://doi.org/10.1016/j.jmb.2015.11.014>
- Roos, W. H., Bruinsma, R., & Wuite, G. J. L. (2010). Physical virology. *Nature Physics*, 6, 733. <https://doi.org/10.1038/nphys1797>
- Roos, W. H., Gertsman, I., May, E. R., Brooks, C. L., 3rd, Johnson, J. E., & Wuite, G. J. (2012). Mechanics of bacteriophage maturation. *Proceedings of the National Academy of Sciences of the United States of America*, 109(7), 2342–2347. <https://doi.org/10.1073/pnas.1109590109>
- Ruigrok, R. W., Crepin, T., & Kolakofsky, D. (2011). Nucleoproteins and nucleocapsids of negative-strand RNA viruses. *Current Opinion in Microbiology*, 14(4), 504–510. <https://doi.org/10.1016/j.mib.2011.07.011>
- Sakamoto, Y., Yamada, G., Mizuno, M., Nishihara, T., Kinoyama, S., Kobayashi, T., ... Nagashima, H. (1983). Full and empty particles of hepatitis B virus in hepatocytes from patients with HBsAg-positive chronic active hepatitis. *Laboratory Investigation*, 48(6), 678–682.
- Saugar, I., Irigoyen, N., Luque, D., Carrascosa, J. L., Rodriguez, J. F., & Caston, J. R. (2010). Electrostatic interactions between capsid and scaffolding proteins mediate the structural polymorphism of a double-stranded RNA virus. *The Journal of Biological Chemistry*, 285(6), 3643–3650. <https://doi.org/10.1074/jbc.M109.075994>

- Schneemann, A. (2006). The structural and functional role of RNA in icosahedral virus assembly. *Annual Review of Microbiology*, *60*, 51–67. <https://doi.org/10.1146/annurev.micro.60.080805.142304>
- Shakeel, S., Dykeman, E. C., White, S. J., Ora, A., Cockburn, J. J. B., Butcher, S. J., ... Twarock, R. (2017). Genomic RNA folding mediates assembly of human parechovirus. *Nature Communications*, *8*(1), 5. <https://doi.org/10.1038/s41467-016-0011-z>
- Sikkema, F. D., Comellas-Aragones, M., Fokkink, R. G., Verduin, B. J., Cornelissen, J. J., & Nolte, R. J. (2007). Monodisperse polymer-virus hybrid nanoparticles. *Organic & Biomolecular Chemistry*, *5*(1), 54–57. <https://doi.org/10.1039/b613890j>
- Singaram, S. W., Garmann, R. F., Knobler, C. M., Gelbart, W. M., & Ben-Shaul, A. (2015). Role of RNA branchedness in the competition for viral capsid proteins. *The Journal of Physical Chemistry B*, *119*(44), 13991–14002. <https://doi.org/10.1021/acs.jpcc.5b06445>
- Sivanandam, V., Mathews, D., Garmann, R., Erdemci-Tandogan, G., Zandi, R., & Rao, A. L. (2016). Functional analysis of the N-terminal basic motif of a eukaryotic satellite RNA virus capsid protein in replication and packaging. *Scientific Reports*, *6*, 26328. <https://doi.org/10.1038/srep26328>
- Snijder, J., Radtke, K., Anderson, F., Scholtes, L., Corradini, E., Baines, J., ... Roos, W. H. (2017). Vertex-specific proteins pUL17 and pUL25 mechanically reinforce herpes simplex virus capsids. *Journal of Virology*, *91*(12), 1–8. <https://doi.org/10.1128/JVI.00123-17>
- Snijder, J., Reddy, V. S., May, E. R., Roos, W. H., Nemerow, G. R., & Wuite, G. J. (2013). Integrin and defensin modulate the mechanical properties of adenovirus. *Journal of Virology*, *87*(5), 2756–2766. <https://doi.org/10.1128/JVI.02516-12>
- Snijder, J., Uetrecht, C., Rose, R. J., Sanchez-Eugenía, R., Marti, G. A., Agirre, J., ... Roos, W. H. (2013). Probing the biophysical interplay between a viral genome and its capsid. *Nature Chemistry*, *5*(6), 502–509. <https://doi.org/10.1038/nchem.1627>
- Speir, J. A., Munshi, S., Wang, G., Baker, T. S., & Johnson, J. E. (1995). Structures of the native and swollen forms of cowpea chlorotic mottle virus determined by X-ray crystallography and cryo-electron microscopy. *Structure*, *3*(1), 63–78.
- Stannard, L. M., & Hodgkiss, M. (1979). Morphological irregularities in Dane particle cores. *The Journal of General Virology*, *45*(2), 509–514. <https://doi.org/10.1099/0022-1317-45-2-509>
- Steele, J. F. C., Peyret, H., Saunders, K., Castells-Graells, R., Marsian, J., Meshcheriakova, Y., & Lomonosoff, G. P. (2017). Synthetic plant virology for nanobiotechnology and nanomedicine. *WIREs Nanomedicine and Nanobiotechnology*, *9*(4), 1–18. <https://doi.org/10.1002/wnan.1447>
- Stewart, H., Bingham, R. J., White, S. J., Dykeman, E. C., Zothner, C., Tuplin, A. K., ... Harris, M. (2016). Identification of novel RNA secondary structures within the hepatitis C virus genome reveals a cooperative involvement in genome packaging. *Scientific Reports*, *6*, 22952. <https://doi.org/10.1038/srep22952>
- Twarock, R., Bingham, R. J., Dykeman, E. C., & Stockley, P. G. (2018). A modelling paradigm for RNA virus assembly. *Current Opinion in Virology*, *31*, 74–81. <https://doi.org/10.1016/j.coviro.2018.07.003>
- Twarock, R., Leonov, G., & Stockley, P. G. (2018). Hamiltonian path analysis of viral genomes. *Nature Communications*, *9*(1), 2021. <https://doi.org/10.1038/s41467-018-03713-y>
- Twarock, R., & Stockley, P. G. (2019). RNA-mediated virus assembly: Mechanisms and consequences for viral evolution and therapy. *Annual Review of Biophysics*, *48*(1), 495–514. <https://doi.org/10.1146/annurev-biophys-052118-115611>
- Uetrecht, C., Barbu, I. M., Shoemaker, G. K., van Duijn, E., & Heck, A. J. (2011). Interrogating viral capsid assembly with ion mobility-mass spectrometry. *Nature Chemistry*, *3*(2), 126–132. <https://doi.org/10.1038/nchem.947>
- Uetrecht, C., Versluis, C., Watts, N. R., Roos, W. H., Wuite, G. J., Wingfield, P. T., ... Heck, A. J. (2008). High-resolution mass spectrometry of viral assemblies: Molecular composition and stability of dimorphic hepatitis B virus capsids. *Proceedings of the National Academy of Sciences of the United States of America*, *105*(27), 9216–9220. <https://doi.org/10.1073/pnas.0800406105>
- Vahey, M. D., & Fletcher, D. A. (2019). Low-fidelity assembly of influenza A virus promotes escape from host cells. *Cell*, *176*(3), 678. <https://doi.org/10.1016/j.cell.2019.01.009>
- Valbuena, A., & Mateu, M. G. (2015). Quantification and modification of the equilibrium dynamics and mechanics of a viral capsid lattice self-assembled as a protein nanocoating. *Nanoscale*, *7*(36), 14953–14964. <https://doi.org/10.1039/c5nr04023j>
- van der Schoot, P., & Zandi, R. (2013). Impact of the topology of viral RNAs on their encapsulation by virus coat proteins. *Journal of Biological Physics*, *39*(2), 289–299. <https://doi.org/10.1007/s10867-013-9307-y>
- van Rosmalen, M. G. M., Li, C., Zlotnick, A., Wuite, G. J. L., & Roos, W. H. (2018). Effect of dsDNA on the assembly pathway and mechanical strength of SV40 VP1 virus-like particles. *Biophysical Journal*, *115*(9), 1656–1665. <https://doi.org/10.1016/j.bpj.2018.07.044>
- van Rosmalen, M. G. M., Nemerow, G. R., Wuite, G. J. L., & Roos, W. H. (2018). A single point mutation in precursor protein VI doubles the mechanical strength of human adenovirus. *Journal of Biological Physics*, *44*(2), 119–132. <https://doi.org/10.1007/s10867-017-9479-y>
- Wang, J. C., Mukhopadhyay, S., & Zlotnick, A. (2018). Geometric defects and icosahedral viruses. *Viruses*, *10*(1), 1–9. <https://doi.org/10.3390/v10010025>
- Yang, L., & Lu, M. (2018). Small molecule inhibitors of hepatitis B virus nucleocapsid assembly: A new approach to treat chronic HBV infection. *Current Medicinal Chemistry*, *25*(7), 802–813. <https://doi.org/10.2174/0929867324666170704121800>
- Yoffe, A. M., Prinsen, P., Gopal, A., Knobler, C. M., Gelbart, W. M., & Ben-Shaul, A. (2008). Predicting the sizes of large RNA molecules. *Proceedings of the National Academy of Sciences of the United States of America*, *105*(42), 16153–16158. <https://doi.org/10.1073/pnas.0808089105>
- Zandi, R., van der Schoot, P., Reguera, D., Kegel, W., & Reiss, H. (2006). Classical nucleation theory of virus capsids. *Biophysical Journal*, *90*(6), 1939–1948. <https://doi.org/10.1529/biophysj.105.072975>

- Zhou, J., Kondylis, P., Haywood, D. G., Harms, Z. D., Lee, L. S., Zlotnick, A., & Jacobson, S. C. (2018). Characterization of virus capsids and their assembly intermediates by multicycle resistive-pulse sensing with four pores in series. *Analytical Chemistry*, *90*(12), 7267–7274. <https://doi.org/10.1021/acs.analchem.8b00452>
- Zimmern, D. (1977). The nucleotide sequence at the origin for assembly on tobacco mosaic virus RNA. *Cell*, *11*(3), 463–482. [https://doi.org/10.1016/0092-8674\(77\)90065-4](https://doi.org/10.1016/0092-8674(77)90065-4)
- Zimmern, D., & Butler, P. J. G. (1977). The isolation of tobacco mosaic virus RNA fragments containing the origin for viral assembly. *Cell*, *11*(3), 455–462. [https://doi.org/10.1016/0092-8674\(77\)90064-2](https://doi.org/10.1016/0092-8674(77)90064-2)
- Zlotnick, A. (2004). Viruses and the physics of soft condensed matter. *Proceedings of the National Academy of Sciences of the United States of America*, *101*(44), 15549–15550. <https://doi.org/10.1073/pnas.0406935101>
- Zlotnick, A., Aldrich, R., Johnson, J. M., Ceres, P., & Young, M. J. (2000). Mechanism of capsid assembly for an icosahedral plant virus. *Virology*, *277*(2), 450–456. <https://doi.org/10.1006/viro.2000.0619>
- Zlotnick, A., Porterfield, J. Z., & Wang, J. C. (2013). To build a virus on a nucleic acid substrate. *Biophysical Journal*, *104*(7), 1595–1604. <https://doi.org/10.1016/j.bpj.2013.02.005>

How to cite this article: Buzón P, Maity S, Roos WH. Physical virology: From virus self-assembly to particle mechanics. *WIREs Nanomed Nanobiotechnol*. 2020;12:e1613. <https://doi.org/10.1002/wnan.1613>